KODAIKANAL OBSERVATORY BULLETINS

Volume 4

1984

INDIAN INSTITUTE OF ASTROPHYSICS
Bangalore

Magnetic Field – Plasma Interaction on the Sun

Proceedings of the Colloquium held on January 23, 1984
at Kodaikanal in commemoration of the 75th Anniversary
of the discovery of the Evershed Effect.

Edited by
K. R. SIVARAMAN
and
P. K. RAJU

Indian Institute of Astrophysics
Bangalore
India

INDIAN INSTITUTE OF ASTROPHYSICS, BANGALORE
1984

Front cover :

Kodaikanal Observatory

The tiled roof building on the left houses the spectroheliographs in operation since the time of John Evershed and bears a plaque at the entrance announcing the discovery of the Evershed Effect on January 5, 1909. On the right extreme is the new Solar Tower Telescope.

(Photograph by K. R. Sivaraman)

JOHN EVERSHED F.R.S. (1864-1956)

CONTENTS

Preface vii

List of Participants ix

Message
M.G.K. Menon xi

Welcoming Address
J.C. Bhattacharyya xiii

SUNSPOT AND ASSOCIATED LOCAL PHENOMENA

The Rotation of the Sun from Mount Wilson Sunspot Measurements
Robert Howard and Peter A.Gilman 1

Line Asymmetry and Magnetic Fields
William Livingston 7

Observations of the Evershed Effect - Past and Present
K.R.Sivaraman 11

Convection and the Phenomenon of Kilogauss Magnetic Fields on the Sun
P.Venkatakrishnan 19

LARGE SCALE AND GLOBAL PHENOMENA

Solar Dynamo Problem
M.H.Gokhale 25

Vector Magnetic Fields in Prominences: Observations and Analysis
R.N.Smartt and L.L.House 35

Modelling of Plasma Structures in the Solar Atmosphere
Vinod Krishan 43

Observations on the Fine Structures in the Solar Decametric Radio Emissions
N.Gopalswamy, G.Thejappa and Ch.V.Sastry 47

Concluding Discussion
Robert Howard 55

PREFACE

The one day colloquium "Magnetic Field - Plasma Interaction on the Sun" was organised at Kodaikanal on January 23, 1984, where the main solar research facilities of the Indian Institute of Astrophysics exist and most important, the place where John Evershed F.R.S. lived and worked for seventeen years. It was on January 5, 1909, seventy five years ago, that he discovered the radial motion of the solar plasma in the penumbral regions of sunspots, which was the first visible demonstration of the interaction of plasma with magnetic field. Originally, the title of this colloquium was planned to be "Evershed Effect", but subsequently it was changed to the present one to provide a wider scope so as to cover a range of allied phenomena on the Sun.

The entire financial support to organise this colloquium and to bring out these proceedings as a special issue of the Kodaikanal Observatory Bulletin was provided by Prof. J.C.Bhattacharyya, Director, Indian Institute of Astrophysics and we would like to express our gratitude to him. We thank the authors as well as the participants who have contributed to the colloquium. Dr. S.P.Bagare with the staff at the Kodaikanal mountain contributed in many ways to the local arrangements. He also helped us in editing the manuscripts. Miss K.Padmavathi did the entire typing work and Mr. R.Krishnamoorthy made the camera ready copies of the manuscripts and was also personally responsible for the printing and preparation of the proceedings in their final form. We acknowledge with pleasure the valuable and devoted services of all these individuals, which have made this mission a success.

Bangalore, December 1984

K.R. Sivaraman

P.K. Raju

LIST OF PARTICIPANTS

P.S.M. ALEEM, Indian Institute of Astrophysics, Kodaikanal.

S.P. BAGARE, Indian Institute of Astrophysics, Kodaikanal.

K.S. BALASUBRAMAINIAM, Indian Institute of Astrophysics, Bangalore.

J.C. BHATTACHARYYA, Indian Institute of Astrophysics, Bangalore.

M.H. GOKHALE, Indian Institute of Astrophysics, Bangalore.

N. GOPALSWAMY, Indian Institute of Astrophysics, Bangalore.

S.S. GUPTA, Indian Institute of Astrophysics, Kodaikanal.

P.S. HAMEED, Indian Institute of Astrophysics, Kodaikanal.

R. HOWARD, National Solar Observatory, Tucson, Arizona.

R. KARIYAPPA, Indian Institute of Astrophysics, Bangalore.

D. KARUNAKARAN, Indian Institute of Astrophysics, Kodaikanal.

V. KRISHAN, Indian Institute of Astrophysics, Bangalore.

W. LIVINGSTON, National Solar Observatory, Tucson, Arizona.

B.S. NAGABHUSHANA, Indian Institute of Astrophysics, Kodaikanal.

L. PETER, Indian Institute of Astrophysics, Kodaikanal.

K.C.A. RAHEEM, Indian Institute of Astrophysics, Bangalore.

P.K. RAJU, Indian Institute of Astrophysics, Bangalore.

K.B. RAMESH, Indian Institute of Astrophysics, Kodaikanal.

K. SASIDHARAN, Indian Institute of Astrophysics, Kodaikanal.

K. SINHA, Uttar Pradesh State Observatory, Nainital.

K.R. SIVARAMAN, Indian Institute of Astrophysics, Bangalore.

R.N. SMARTT, National Solar Observatory, Sunspot, New Mexico.

P. VENKATAKRISHNAN, Indian Institute of Astrophysics, Bangalore.

K. SUNDARARAMAN, Indian Institute of Astrophysics, Kodaikanal.

J.V.S. VISWESWARARAO, Indian Institute of Astrophysics, Kodaikanal.

सत्यमेव जयते

सदस्य
योजना आयोग,
योजना भवन
नई दिल्ली-110001
MEMBER
PLANNING COMMISSION
YOJANA BHAVAN
NEW DELHI-110001

January 20, 1984

MESSAGE

I am very happy to learn about the Colloquium being arranged at Kodaikanal on the occasion of the 75th anniversary of the discovery of the Evershed effect. The contributions of John Evershed to the development of the Kodaikanal Observatory are overwhelming. He equipped the Solar Physics Laboratory with fine instruments, almost entirely built with his own hands. The high resolution spectroheliograph set up by him at Kodaikanal was instrumental in arriving at answers to some vital questions about the gases forming sunspots. His discovery opened up a new area in our understanding of the physics of the sun.

Over these past seventyfive years we have moved into many new areas of this fascinating subject. More details of the interactions of solar plasma with the magnetic field have come to light. Deeper thinking aimed at unveiling the energetic processes happening in the solar atmosphere are now called for. I hope that the discussions will open new pathways to future investigations as the discovery by Evershed has done 75 years ago.

I wish the Colloquium all success.

MGK Menon 20/1/84

(M.G.K. Menon)
Chairman, Governing Council
Indian Institute of Astrophysics

WELCOMING ADDRESS

J.C. Bhattacharyya
Indian Institute of Astrophysics
Bangalore 560034
INDIA

Friends and Colleagues,

I welcome you all to Kodaikanal and to this Observatory; I wish to express my gratitude to all the individuals who have come inspite of their heavy pressure of work; my special thanks to our friends from abroad, who have been generous enough to accommodate this visit in their very tight schedule.

The purpose of today's gathering is to discuss some aspects of study of the physics of the sun; the occasion is to commemorate a discovery which was achieved in this Observatory three quarters of a century ago. On your way up here, you might have noticed a plaque on the wall of a building indicating the event. I shall try to give a little history of the human efforts which culminated in the unfolding of one of nature's mysteries.

Prof. M.G.K.Menon, Chairman of the Governing council of this Institute was very keen about arranging this meeting. He had planned to attend the meeting but unfortunately, the extreme load of his responsibilities have prevented him from coming here today. He has, however, sent his message on this occasion.

Let me start from the very beginning. In the last decade of the eighteenth century, a small observatory was started by the British East India Company in the outskirts of the settlement around Fort St. George which has now grown to be the cosmopolitan city of Madras. They had, among other instruments, a transit instrument which was mounted on a granite pillar. On the four sides of the pillar, the founders decided to leave a message to the posterity. Inscribed in four languages, Latin, Tamil, Telugu and Urdu, known at that time as Hindustani, the pillar still proclaims the historic event. Translated into English the message reads: "Posterity may be informed a thousand years hence, where the seeds of Mathematical sciences were planted by the British liberality in Asia".

The dreams of the founders were not in vain, as shown by the course of events which followed. Under the inspired direction of some devoted astronomers, the Madras Observatory indeed blossomed into an active centre of astronomical research. Names of Taylor and Goldingham may be mentioned, of those who undertook precise determination of positions of several thousand stars. Seven decades later, the helm of affairs passed on to an astronomer whose name is indelibly marked in astronomical literature; Norman Pogson, who took over as the Chief Astronomer of Madras Observatory. He introduced a fresh wave of enthusiasm and encouraged local scientists in the investigation of the heavens. Name of C.Raghunathachari could be mentioned as one among the first Indian astronomers of modern era. Pogson was keen on the study of asteroids. To the list of asteroids, five names, Asia, Sappho, Sylvia, Vera and Camilla were added by his efforts from the Madras Observatory. He put up a strong case for modernization of observing equipment, and to shift the observatory to a more suitable location on the hills.

To cut a long story short, things began to move only after Pogson's death. A location in the Palni hills was selected and the work on construction began in 1899. In 1901, the Kodaikanal Observatory came into existence. The emphasis was now on Astrophysics, the new astronomy. Detailed studies of solar spectra had started giving totally new types of information. Only a few decades ago, something which was considered impossible to know about the celestial objects had suddenly become available in unimaginable detail. Spectroscopy had become the most powerful tool in Astrophysics.

Evershed came into this field at this juncture. In 1905, he left his village home in Surrey in the United Kingdom, where he had built a small but well equipped observatory. He packed up some of the components and brought them with him to Kodaikanal. On his way to India, he travelled via the United States and Japan where he picked up some more components and came fully prepared to start a modern observatory. He had discussed his plans with stalwarts like Pickering, Barnard, Frost and St. John and hence he went straight ahead with his task at Kodaikanal. The spectroheliograph in the next building that you can see today has basically remained in its original configuration designed by Evershed.

This was not the first visit by Evershed to India; he had earlier been with the British team at Talni near Ratnagiri in January 1898 when he first obtained the near Ultraviolet spectra of the Sun. On joining Kodaikanal, the first problem he undertook for investigation was to explain the peculiarities of sunspot spectra. In the course of that work, fortune smiled upon him. On January 5, 1909, after seven days of heavy rain, the sun rose in an unusually clear sky with excellent seeing. Evershed could obtain a series of high resolution spectra across a spot group. The original plate is preserved in this Observatory; we have placed a magnified image of the plate in the spectroheliograph room. By employing the method of photographic subtraction, largely developed by him, he could get clear indications of systematic Doppler shifts in the spot regions. One of the nagging questions about the dynamical structure of sunspots began to clear up.

That was the beginning of a series of investigations, which unfolded the system of complex flow around sunspot regions. Since then it has been a long journey along the path of discoveries in many observatories, connecting the plasma interactions with magnetic field, small scale velocity fields, large supergranular motions, and many other features displaying an infinite variety of plasma dynamics in the solar envelope.

The problem has not been completely solved today. No scientific discoveries clear a problem completely. They give deeper insights into nature's processes and we come across fresh problems of a more refined variety. There are several aspects of the phenomena which remain as enigmatic as ever. We have chosen today to have a general reconnaisance of the progress so far made in this field and of the problems we face today. We hope to obtain some ideas regarding the immediate steps needed and therefore to readjust the course of future investigations in this field. We shall now begin with the scientific papers.

Kodaikanal Obs. Bull. (1984) 4, 1-5.

THE ROTATION OF THE SUN FROM MOUNT WILSON SUNSPOT MEASUREMENTS

Robert Howard *
Mount Wilson and Las Campanas Observatories
Carnegie Institution of Washington

and

Peter A. Gilman
High Altitude Observatory
National Center for Atmospheric Research**.

1. Introduction

We have recently completed the measurement and reduction of 62 years of white-light solar images taken at the Mount Wilson Observatory. So far the data have been analyzed for differential rotation and time variations of this quantity, among other parameters. The data, the measurement and reduction techniques, and the results obtained so far are described in two publications: (Howard, Gilman, and Gilman, 1984; Gilman and Howard, 1984). This is a brief review of that work.

The interval covered by these data is 1921-1982. The measurements were carried out in an interval of two years by Pamela Gilman. The homogeneity in the reduction and in the observations themselves are two advantages of these measured spot positions over other data. A further advantage of this analysis —— and a characteristic that distinguishes it from nearly all previous work —— is that measurements were made of individual sunspots, not just sunspot groups.

2. Data

The white-light solar images have been obtained with the same focal-plane shutter mechanism at the 60-foot tower telescope at Mount Wilson throughout the interval. The 18.3 m focal length lens now in use was originally installed about 1916. The coelostat mirrors were replaced twice during the interval.

The image diameter is 170 mm. Pole markers on the images designate the axis of the solar rotation. The focal-plane shutter gives an exposure time of about 1/1000 second for the f/60 beam. The observing log contains the time and data of each observations, the focus setting, temperature and other information.

3. The Measurements

An electronic measuring pad placed over a light box was used for position measures on the plates in two dimensions. The accuracy of such measurements is about 0.1 mm, which is about one arc sec on the plates.

Each plate was positioned on the tablet with the rotation axis of the sun aligned with one axis of the tablet. The limb was defined by 8 equally spaced measurements. Then each spot umbra (penumbrae were not

---

[*] Now at National Solar Observatory, Tucson, Arizona, U.S.A. Operated by the Association of Universities for Research in Astronomy, Inc. under contract with the National Science Foundation.

[**] The National Center for Atmospheric Research is sponsored by the National Science Foundation.

mesured) was measured with two position measures of the cross-hair. This enabled us to calculate the position and approximate area of each spot.

Altogether nearly 15,000 usable images were obtained in the 62-year interval. Nearly 335,000 daily sunspots were measured on these plates.

Only sunspot umbrae were measured in this program because we felt that they represented the fundamental positions and areas of the spots.

4. The Analysis

Rotation rates of individual sunspots were determined only from one-day differences of longitude mesurements. In order to identify individual sunspots from one day to the next using a computer program, which is a difficult task even when done by eye on a small sample of spots, we first grouped the spots **into** sunspot groups by proximity. Then we determined the identification of groups from one day to the next. The final step was to match spots within the group on two consecutive days using a technique which maximized the number of spot coincidences within a number of possible relative orientations (excluding rotation of the group) in a two-dimensional grid. This method turned out to be insensitive to the assumed rotation used to pick the group associations.

Altogether nearly 36,000 groups were identified on the next day, and from these 96,283 sunspots were identified as next-day returns. The method is quite conservative as is shown by the fact that only 29% of spots were defined as returning the next day, and 10.5% of the groups seen the following day contained no spots defined as returns.

The spot group and individual spot rotation rates discussed in this paper are sidereal rates.

5. Results

The spot group rotation rate determined for the whole data set is:

$$\omega = 14.393\ (\pm 0.010) - 2.946\ (\pm 0.090) \times \mathrm{Sin}^2 B \text{ deg day}^{-1},$$

where B is the heliographic latitude. For all spots we obtained

$$\omega = 14.522\ (\pm 0.004) - 2.840\ (\pm 0.043) \times \mathrm{Sin}^2 B \text{ deg day}^{-1}.$$

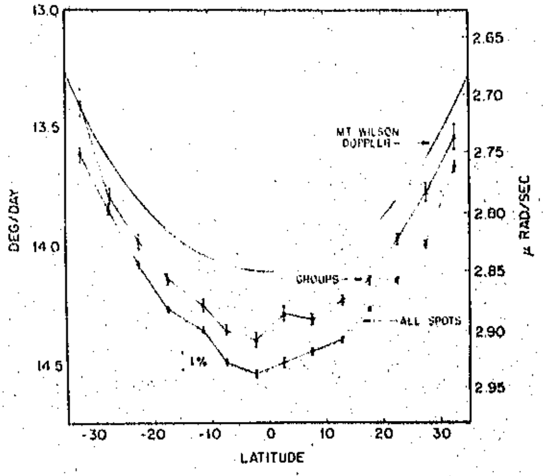

Fig.1. Rotation rates for all sunspots and for sunspot groups are plotted for 5-degree latitude zones. These results refer to the interval 1921 to 1982. Also plotted is the Doppler sunspot rate determined from the Mount Wilson data for the interval 1967 to 1982 (Howard et al., 1983), corrected for a small dispersion error (Snodgrass et al., 1984). The Doppler data are plotted from the smooth series expansion.

Figure 1 shows the rotation rate of sunspots and groups as a function of latitude. Also shown for comparison is the Doppler rate determined from the Mount Wilson magnetograph data for the interval 1967-1982 (Howard et al. 1983).

For the largest sunspots (area > 15 millionths of the hemisphere) the rotation may be expressed

$$\omega = 14.282\ (\pm 0.018) - 2.636\ (\pm 0.169) \times \sin^2 B \text{ deg day}^{-1}.$$

For medium sized spots (5 < area < 15)

$$\omega = 14.439\ (\pm 0.010) - 2.616\ (\pm 0.088) \times \sin^2 B \text{ deg day}^{-1},$$

and for the smallest spots (area < 5)

$$\omega = 14.549\ (\pm 0.005) - 2.869\ (\pm 0.051) \times \sin^2 B \text{ deg day}^{-1}.$$

The rotation rates of the sunspots of various sizes as a function of spot size are shown in Figure 2.

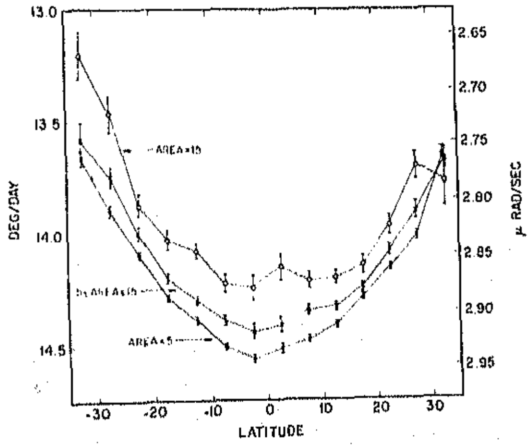

Fig.2. The rotation rate of spots of various sizes as a function of latitude. The zones are 5 degrees in width.

Variations of the average sunspot rotation rate are seen which correlate with phase in the activity cycle. There is strong peak in rotation near sunspot minimum and a weaker peak near sunspot maximum. A similar pattern is seen in Mount Wilson Doppler rotational velocity data, which is available starting in 1967. There are at times small phase shifts between the peaks seen in the two data sets.

The amplitude of the sunspot rotation variations is about 0.5% day^{-1} or about 3-4% of the average equatorial rotation rate. The amplitude of the Doppler variations is nearly double that value: 0.6 - 0.7 deg day^{-1}, or 4-5% of the average equatorial rate.

6. Discussion

The variation of rotation rate with spot size is a puzzling result. Ward (1966) found a similar result for spot groups of various sizes using the Greenwich data. The difference between the largest spots and the smallest spots in this study is nearly 2%. One possible explanation for this effect is that all spots rotate at the same rate at some depth where they are linked to subsurface flux ropes, but that the larger spots experience more viscous drag than do the smaller spots due to their larger cross-section as they move through the photospheric plasma. We tested this hypothesis by examining rates during years when the spot-plasma rate difference was large and years when this difference was small. We could find no significant difference between the rotation rate differences of large and small spots in these two samples. This implies either that viscous drag is not a significant factor in determining the rotation rates of sunspots or that the viscous drag is the same for spots of all sizes.

In recent years there has been some debate about whether or not the sunspots and the photospheric plasma rotate at the same rate. Although this analysis does not give new results concerning the Doppler rates, it does not make it evident that the plasma cannot rotate at the same rate as all the spots.

In absolute terms, our rotation rate for spot groups is about 1% slower than that found by Ward (1966) and coincides closer than 0.1% with that found by Newton and Nunn (1951). The reason for these agreements is that Ward's results refer to all spot groups from positions that were not area-weighted (Greenwich). These results, therefore tend to be influenced by the smaller spots, which, as we found, rotate faster than the larger spots. Newton and Nunn used single-spot groups, which tend to represent large spots. Since our group positions are area-weighted, they represent the rotation of the largest spots, hence the agreement with Newton and Nunn is good.

The cycle-related amplitude variations of the sunspot rotation rate imply periodic angular momentum exchange with deeper layers in the sun. This exchange cannot take place with other latitudes at the solar surface because such large amplitude fluctuations are not seen in the Doppler data (Howard, 1976). Nor can the momentum be exchanged with the gas above the photosphere, because the inertia of this material is so low. We presume that the magnetic flux tubes of the spots are linked to deeper layers which share more or less in the same phase the variations seen in the photosphere. Alternatively the deeper layers at which the spots are linked may show no variations, and the surface rate of the spots may be determined by the drag imposed by the surface plasma.

In any case the rotation variations may be considered to represent yet another mode of torsional oscillation of the sun. These motions represent a somewhat higher amplitude torsional oscillation than those discovered earlier (Howard and LaBonte, 1980; LaBonte and Howard, 1982). The sun seems easily excited in torsional modes.

References

Gilman, P.A., and Howard, R., 1984, Astrophys. J., **283**, 385.

Howard, R., 1976, Astrophys. J. (letters), **210**, L 159.

Howard, R., Adkins, J.M., Boyden, J.E., Cragg, T.A., Gregory, T.S., LaBonte, B.J., Padilla, S.P., and Webster, L., 1983, Solar Phys. **83**, 321.

Howard, R., Gilman, P.A., and Gilman, P.I., 1984, Astrophys. J. **283**, 373.

Howard, R., and LaBonte, B.J., 1980, Astrophys. J. (letters), **239**, L 33.

LaBonte, B.J., and Howard, R., 1982, Solar Phys. **75**, 161.

Newton, H.W., and Nunn, M.L., 1951, M.N.R.A.S. **111**, 413.

Snodgrass, H.B., Howard, R., and Webster, L., 1984, Solar Phys. **90**, 199.

Ward, F., 1966, Astrophys. J. **145**, 416.

DISCUSSION:

SIVARAMAN: When the spot is near the limb there will be foreshortening. This could result in the over estimation of longitude by more than 1/2°. How did you take care of this?

HOWARD: We did not measure spots that were more distant than 60° from the central meridian.

SIVARAMAN: You need torsional oscillations to explain your spot rotation. How will this fit in with the rotation rate above the sunspot zone?

HOWARD: From the Doppler measure we find that the high latitudes share in the rotational modulation of the sunspot zones.

GOKHALE: Is the variation of the rotation of spot groups in agreement with torsional oscillation from Dopplergram?

HOWARD: No. The effect described has an amplitude several times that of the torsional oscillation. We have made a preliminary search for the torsional oscillation effect in our data with no success.

BAGARE: Would it be possible to study from your data, the occurence of retardation in proper motion of the spot groups as reported by Waldmeir?

HOWARD: Probably yes, we have to analyse the data in order to look for these.

VINOD KRISHAN: Is the missing penumbrae of some of the spots due to the overlapping of different spots in a sunspot group?

HOWARD: I don't believe that the reason for missing penumbrae is known for certain. It is most likely due to the magnetic configuration within the spot group, which may or may not involve a nearby sunspot.

BALASUBRAMANIAM: Is there any correlation between the area of the spot and the latitude? How do you account for areas of merging spots? Once the merger/coalition starts, is there any relation between the merger time and rotation rate?

HOWARD: We have not looked for such an effect yet. When comparing the position of individual spots from one day to the next, we allow only one agreement for a spot. Thus, when we try to lineup second of the merged spots on the next day, there is no spot to associate it with. We have not studied this aspect as yet.

ALEEM: Could you please explain the modern method of measuring the area of sunspot?

HOWARD: Our techniques is designed for speed of measurement rather than accuracy. We place the cross-hair of our measuring instrument at two positions, which are digitized and stored for later analysis. These two positions are chosen so that 1) one arm of the cross-hair points to the disk center and 2) the area of the quadrilateral defined by the two cross-hair positions approximate that the sunspot umbra. We estimate our accuracy as about 30% for a single umbral measurement.

Kodaikanal Obs. Bull. (1984) 4, 7-9.

LINE ASYMMETRY AND MAGNETIC FIELDS

William Livingston
National Solar Observatory *
Tucson, Arizona
U.S.A

1. Introduction

The measurement of the asymmetries of Fraunhofer lines shows promise as a diagnostic of convection at the surface layers of the sun and stars. We discuss today the observational evidence that line asymmetry, and by inference granular convection, is inhibited by surface magnetism.

2. Origins of Line Asymmetry

St. John, working at the Mt. Wilson 150-ft tower in the first decades in the 1900s, discovered what he termed a 'Limb Effect'; weak to moderate strength Fraunhofer lines display a red shift near the limb, and the amount of this shift is greater for the weaker lines. This 'Limb Effect' can now be understood as a consequence of granulation velocities and as such, is more correctly thought of as a "Centre-disk effect". High resolution spectra at disk centre indicate that the bright granules are rising relative to the darker intergranular space, the material of which is falling. Low resolution spectra, which average over many granules, then possess a brightness weighted blue shift at disk centre which disappears at the limb because the motions are predominately radial.

A solar granule may be considered as a convection cell. In the centre is a rising column of hot gas moving slowly from deep down, accelerating near the surface to conserve mass, radiating energy and thus cooling, then turning over and flowing down around the cell boundaries. A moderately strong absorption line, such as FeI 5303 Å, is formed throughout the granular layers. As a result the extreme wings of the line, which sense the deepest slow moving layers are relatively undisplaced compared to its main body. Likewise the line core is undisplaced because it is formed well above the granular cell where all outward motion has ceased. A plot of the bisector of such line has a resulting C- shape. Displacement of the extreme of the middle part of the C from its toe can be taken as a measure of convective vigour.

Distortion of the C - shape can arise from line blends, atomic fine structure and an unsymmetric instrument profile (Dravins, et al. 1981). All Fraunhofer lines are in fact blended to some degree. By carefully selecting lines that are minimally blended and then averaging many comparable lines together we obtain a meaningful bisector. Atomic fine structure is avoided by confining ourselves to iron lines. Finally the 1-meter Fourier Transform Spectrometer (FTS) has a demonstrated symmetric profile and exhibits very low noise so far as line bisectors are concerned.

---

* Operated by the Association of Universities for Research in Astronomy, Inc. under contract with the National Science Foundation.

The stochastic nature of granulation is dealt with by spatial averaging. A field of 2 arc-minutes is useful for defining the variation of line asymmetry across the solar disk. Ultimate averaging is the entire disk (10^5-10^6 granules). The internal scatter in full disk FTS bisectors corresponds to about 2 $m.s^{-1}$.

3. Influence of Magnetic Fields on C-shapes

Observational evidence - the 'abnormal granulation' near sunspots - plus theoretical prediction prompts us to investigate how C - shapes are affected by ambient magnetic fields. FTS observations at 2 arc-min resoluion made in plage areas and in quiet areas for comparison at the same limb distance indicate that the bisector amplitude (wing-core) is always reduced in the plage. The only exceptions to this rule occur very near the limb where the amplitude may or may not be reduced.

4. Variability of Line Asymmetry with the Solar Cycle

Two data sets have been examined for the temporal variability of the C - shapes (Livingston, 1982). The profile of FeI 5250.6 Å has been studied for the years 1976-1981 using material acquired with the 13.5-m spectrograph. Because such spectrometer observations are relatively noisy (~ 50 $m.s^{-1}$) many days must be averaged together, but when this is done the position of mid-C relative to the core is seen to have diminished by ~2m Å over these years of rising activity. Beginning in May 1980, FTS profiles became available. The noise in C - shapes from the FTS is much less ~ 5 $m.s^{-1}$. FTS archives for several strong Fe lines indicate a continuation of the trend found with the spectrograph through 1982. During 1983 the C - shapes began to strengthen.

5. Comment on the Pic-du-midi Results

Macris and Rösch (1983) examined the very best white light granulation photographs obtained in recent years at Pic-du-midi. The average size of the granulation was deduced by measuring the average intergranule distance. Tentatively they find that granule size becomes smaller with increasing solar activity.

6. Conclusions

Full disk line asymmetry which is a signature of granular convection has been observed to be diminishing with time until recently when the trend apparently reversed. A comparison of low spatial resolution plage vs quiet regions on the solar disk suggests that surface magnetic fields may inhibit line asymmetry. The average size of granulation likewise is reduced by solar activity according to French observers. We conclude that magnetic fields, expanding over the sun's surface from active regions, may interact globally with the solar granulation to significantly alter the transport of energy through this outermost layer.

References

Dravins, D., Lindergrin, L., and Nordlund, A, 1981, Astron. Astrophys. **96**, 345.

Livingston, W.C, 1982, Nature, **297**, 208.

Macris, Rösch, J, 1983, Compt. Rendu, **296**, 265.

DISCUSSION:

BHATTACHARYYA: What is the data from which the French have concluded that the granule size depends on phase in the activity cycle?

LIVINGSTON: They have studied a few (perhaps half a dozen) superior white light photographs taken at Pic-du-midi. Their method involves finding the average distance between granules near disk center in a quiet region.

BALASUBRAMANIAM: Are there any changes in granule size close to spot penumbra?

LIVINGSTON: Although the reference escapes me, I am certain that in the vicinity of active regions, and therefore near penumbrae, one finds "abnormal granulation" which is fragmented compared to normal granulation.

VENKATAKRISHNAN: Can this abnormal granulation be an extension of the inhibition effect in C-shapes due to magnetic fields?

LIVINGSTON: Yes, I assume it is the same mechanism. However, to account for the full disk changes we observe the effect most to be global.

HOWARD: Do the changes in asymmetry seen in integrated light come from the individual plages on the disk?

LIVINGSTON: A good question which I am not prepared to answer quantitatively. As mentioned above, I have been thinking more of a global, rather than active region influence. We do not know that the observed changes in line strength, equivalent width, for example, cannot be caused just by individual plages.

Kodaikanal Obs. Bull. (1984) 4, 11-17.

OBSERVATIONS OF THE EVERSHED EFFECT - PAST AND PRESENT

K.R. Sivaraman
Indian Institute of Astrophysics
Bangalore 560034
INDIA

There exist good reviews on this topic by Schröter (1967) and Maltby (1964). The purpose of the present one on this occasion is to bring out fully the pioneering work of John Evershed in all its aspects in this field and also to update the earlier reviews.

John Evershed (1909a,b,c) while analysing the sunspot spectra obtained by him at Kodaikanal for pressure determination in spots observed that the spectral lines show displacements in the penumbral region of sunspots. This was in fact a remarkable observation since spectroscopic observations of sunspots were started several years earlier, but line displacements were not detected previously in the spectra of the spot penumbrae. The first plate showing this line displacement was exposed on January 5 and 7 in 1909 - 75 years ago - on a spot at latitude 9°N and longitude 31°W of the central meridian covering a region 4650 A to 4790 A with a dispersion of 1.08 mm Å^{-1}. He attributes the unusual amount of detail visible in the spectrum as due to the "clearness and steadiness of the air at the time of the exposure". A preliminary measurement of ten of the best defined lines showed a mean displacement of 0.027 Å (or 0.86 km sec^{-1}) at the outer edges of the penumbra indicating a receding velocity on the limbward side of the spot. He found an approaching velocity of the same magnitude on that part of the penumbra closer to the centre of the disc. Continuing his investigations with 150 spectra representing seven different spots in the northern hemisphere and four in the southern he established the following results:

1. All spots whether in the southern or northern hemisphere show the same amount of line shifts when at the same distance from the centre of the disc and the sense of displacement is to the violet on the side of the penumbra towards the centre of the disc and to the red for the limbward penumbra.
2. These displacements are maximum for spots between 30° and 60° longitudes and disappear when they are within 10° of the centre.

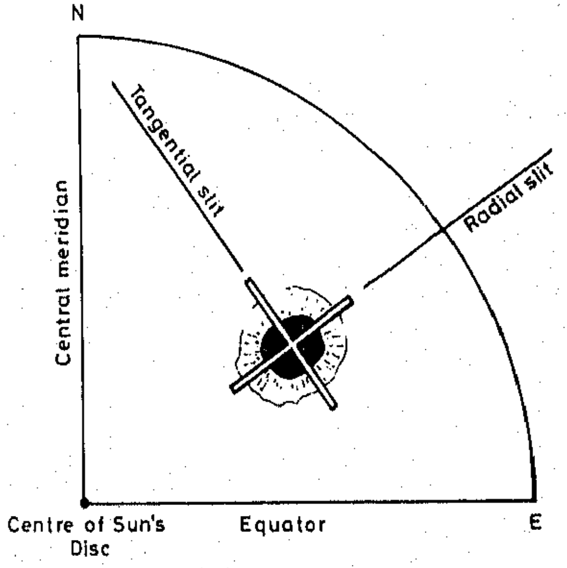

Fig.1. Radial and tangential positions of the spectrograph slit for observing Evershed flow in sunspots.

3. He found maximum line displacements for a radial slit position and no displacement for a slit normal to this position (tangential slit, Figure 1).

These observations convinced Evershed that the displacement of lines was solely due to the Doppler shift caused by the movement of the sunspot gases directed radially and horizontally outwards from the centre of the spot. This radial outflow of solar plasma from sunspots is now known as the Evershed effect. The absence of the tangential velocity ruled out any rotational motion of the gases which conflicted with the concept of motion of gas within the spot by Hale (1908). Evershed (1910) continuing his studies using absorption lines of different strengths found out that strong lines (Rowland Intensity 5-6) show lower velocities ($\sim$1.5 km/sec^{-1}) while faint lines (Rowland Intensity 0-1) show higher velocities (2-3 km sec^{-1}). He also established the monotonic increase of radial velocity from the umbral boundary with a maximum near the outer boundary of the penumbra. Although his earlier studies (1909a,b) showed that the motion abruptly ceases near the periphery of the penumbra, his subsequent observations (1916) gave evidence of the extension of the motion almost 8000 km beyond the penumbral boundary. From his observations using the CaII H & K lines, he showed that there is an inward flow of matter in the spot with a velocity of $\sim$1.8 km sec^{-1}. Evershed also detected tangential component of the velocity of $\sim$3.6 km sec^{-1} in five of the spots he studied and the direction of rotation was counter clockwise for some spots while clockwise for others.

The voluminous work of St. John (1913) using the 60-ft solar tower at the Mt.Wilson Observatory, of measurements of the Evershed velocities of 500 selected lines representing different elements and a large range of excitation potentials confirmed Evershed's earlier findings on faint metallic lines. For the faint lines he observed an outflow of materials from the spot into the undisturbed photosphere, whereas the strong lines (Al and Fe lines) showed no Evershed velocity. For still stronger lines (NaI D_1, D_2, and Mg b_1) and for chromospheric lines there was a reversal in the direction of motion indicating a radial flow of material into the spot (Figure 2).

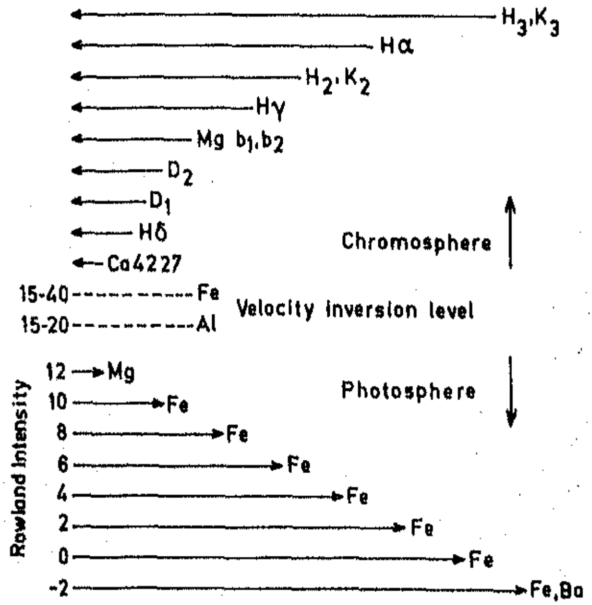

Fig.2. Schematic representation of the height dependence of the Evershed flow. The arrows towards the right represent outflow and the arrows towards the left represent an inflow of material.

This would imply that the material depletion in the umbra due to outflow at the lower levels, is replenished by inflow of material at the chromospheric level. Evershed's (1910) attempts to detect motion in the umbra using the photospheric lines showed surprisingly a descending motion of $\sim$0.4 km sec^{-1}. Abetti's (1932) observations during the sunspot maximum of 1926-1934 showed that the radial velocity varied from 0.2 to 6 km sec^{-1} and in addition there were irregular tangential components in the range 0-5 km sec^{-1}. He also detected that the maximum velocity occurred at the umbra-penumbra boundary and not at the outer edge of the penumbra, which contradicted Evershed's findings. But Abetti's samples belonged to complex spot groups, whereas the measurements of Evershed and St. John pertained to single and rather inactive sunspots. This shows that there may be a clear distinction in the pattern of the flow between the two varieties of spots.

Michard (1951) was the first to relate the outflow velocity with the size of the spot and its magnetic field. He also established an empirical relation for the centre-to-limb variation of the velocity ($V_{r,\theta}$) in terms of the maximum radial velocity ($V_{r,o}$) and the angle (θ) between the line joining the observer and the direction normal to the solar surface by the relation,

$$V_{r,\theta} = V_{r,o} \ (1-0.8 \sin \theta)$$

Later Schröter (1965a) obtained a similar relation

$$V_{r,\theta} = V_{r,o} \ (1-0.3 \sin \theta)$$

This observed centre-to-limb variation confirms the height dependence of the velocity suggested by St.John (Figure 2). Kinman (1952,1953) in his classical work on this topic derived the spatial distribution of velocities over a sunspot from the spectra obtained at the Oxford solar telescope. Assuming cylindrical symmetry about the spot centre he derived the radial, tangential and vertical velocity components from the mean sight-line velocities at many locations within the spot. His investigation covering one large and three small spots showed that the maximum radial velocity attained, increased linearly with umbral size, but the time to reach this maximum velocity was independent of the size of the umbra. The interesting point is that the radial velocity component V_r showed an increase from ~ 1km sec^{-1} at the edge of the umbra and reached a maximum value of ~2 km sec^{-1} at the middle of the penumbra and finally reached zero in the photosphere well outside the spot. But according to Brekke and Maltby (1963) the radial velocities end abruptly at the outer boundary of the penumbra. Schröter's spectra confirm Maltby's findings, but all these as we shall see soon depend to a very large extent on the spatial resolution employed for the observations. The spot velocity fields derived by Holmes (1961) for two spots - one large and another small - using the non Zeeman line Fe I 5576.1 Å showed a maximum radial velocity at the edge of the penumbra with an extended flow reaching zero well beyond, in the photosphere. But the maximum velocity for the large spot was only ~ 0.6 km sec^{-1} as against the velocity of 3.5 km sec^{-1} expected from Kinman's linear relation connecting maximum velocity and spotsize. Also for the large spot, the velocity reaches out far into the photosphere before it becomes indistinguishable. From the measurements of the radial, tangential and vertical velocity components for a spot at six disc positions, Servajean (1961) showed that the maximum radial velocity in spots increased with increments in μ (= Cos θ) values. His interpretation is that the higher layers have lesser radial velocity in spots as compared to the deeper layers. Holmes (1963) also detected a similar variation in the U_{max} as the spot approached the limb, but interpreted this as the effect of scattered light in the telescope which becomes important as the spot is foreshortened at the limb.

High Resolution Observations

Among these mention must be made of observations by Holmes (1961, 1963), Bhatnagar (1964) and Schröter (1965a,b) who used dispersions in the range 5.0 to 8.0 mm/Å for the study of the Evershed phenomena.

Bhatnagar (1964) measured the sight-line velocities on a spot during its successive passage across the disc for various positions on the disc (ranging from μ = 0.35 - 0.95) using non-Zeeman lines (Ni I 4912 Å, Fe I 5576 Å and Fe I 5691 Å). He used the Kodaikanal 120 foot focal length solar tower telescope which has an image scale of 5.5 arc sec mm^{-1} and the associated 60 foot spectrograph at dispersions of ~ 8 mm Å^{-1}. The radial velocities derived by him from the line-of-sight velocities assuming cylindrical symmetry, steeply rose from the umbral border reaching a maximum value of 1.5 - 2.0 km sec^{-1} near mid penumbra and then declined gradually to almost zero far out in the photosphere. Ni I 4912 Å and Fe I 5691 Å showed similar velocities whereas Fe I 5576 Å had systematically lower velocities by about 30-35%. The velocities in all the three line progressively decreased from the centre to the limb, a fact that was noticed by Michard (1951) and Servajean (1961) earlier. This is more pronounced for observations made close to the limb (Holmes, 1963). The straight line fit to the plot of the velocities for different μ positions show that the slopes for the two weak lines 4912 Å and 5691 Å are nearly the same, while the slope is flatter for the strong line 5576 Å. This makes one feel that the velocity dependence with height in the atmosphere may be real, although the scattered light would contaminate the estimation of velocities to a certain extent. Another interesting point in Bhatnagar's velocity measure is that they pertain to the successive passages of the same spot and the fact emerges that the radial velocities are higher in the fully developed phase than in the early phase of growth of the spot.

The existence and the numerical value of the tangential velocities are debatable points. There are as many observations in the literature showing the presence of the tangential velocities as there are pointing to their absence. Evershed (1909c, 1910) detected tangential components of 0.25 to 0.35 km sec^{-1}. However in his later measurements (1916) he found no evidence for a regular tangential component, although irregular velocities were present at times. Kinman (1952) believed that the tangential component was random in nature and in general was within the errors of measurement although at some locations within the spot the value was as much as -0.5 ± 0.2 km sec^{-1}. But his neglect of the tangential component in the interpretation of his later measurements (1953) appears prejudicial. Abetti's (1932) measurements on 26 spots show irregular tangential component with values varying from 0 to 5 km sec^{-1}. Measurements of Servajean (1961) and Bhatnagar (1964) are indecisive and the errors in the latter's measurements are rather large, making a realistic conclusion on the tangential components not possible. Systematic and precise measurements with high spatial and spectral resolution are called for to settle this question.

The use of high spatial resolution and spectral resolution not only made the velocity measurements more precise and error free, but also brought out the microscopic structure of the Evershed flow as motions in the penumbral filaments as well as the phenomenon of asymmetry of spectral lines in the penumbral regions. Bumba (1960) using the high dispersion spectrograph of the Crimean

Observatory detected the strong asymmetry in the line profiles within the penumbra which accompanies the Evershed flow. Servajean (1961) studied the changes in the line asymmetries for different spot positions on the solar disc. Bumba termed this phenomenon the 'line flag' whereas Holmes (1963) who also studied the asymmetry called it the 'line flare'. It is interesting to note that Evershed (1916) detected in his low dispersion spectra that the spectral lines develop a 'diffuse wing' in the direction of the Evershed displacement near the outer boundary of the penumbra. Similar diffuse asymmetric widening was also detected in the spot spectra at the McMath-Hulbert Observatory (1956). But its real significance was brought out only by the work of Bumba and Servajean. Under very favourable seeing conditions, Bumba was even able to resolve the broadening into a satellite line but Servajean, Holmes or Bhatnagar do not find any indications of such a satellite line in their spectra. Bhatnagar (1964) in his photometric study has investigated the dependence of the asymmetry on the strength of the line, on the locations of the slit on the spot and on the spot's position on the disc. The asymmetry grows in magnitude from the edge of the penumbra and reaches maximum values around the middle of the penumbra. The asymmetry has the same sense as the Evershed flow for the three lines he used (4912 Å, 5576 Å and 5691 Å) and probably therefore is independent of the strength of the line. Also, the maximum asymmetry is a function of the spot's position on the disc, such that the spot near the disc centre has an asymmetry maximum smaller than for spots near the limb. Again stronger lines show less of asymmetry than the weaker lines. Bumba finds that the flagging in D_1 and D_2 lines of Na I is opposite to the direction of the Evershed displacement and the direction of flag near the core of these lines is opposite to that in the wings. Servajean (1961) has suggested that the asymmetry is a manifestation of the different velocities corresponding to the different strata in the line forming layers, whereas according to Bumba (1963) the upstreaming of material at the umbral-penumbral boundary which bends and becomes horizontal in the penumbra cause the asymmetry. The asymmetry can also result when the outward moving material in the bright fibrils of the penumbra cause a blue wavelength shift which is not balanced by the inflowing matter in the dark fibrils of the penumbra (Schröter 1965b). Such an asymmetry would give a C-shape to the bisector of the line profile. The C-shape and its change for different μ positions have been investigated in great details by Schröter (1965a) using the Freiburg spot spectra employing the equidensitometry technique. The potentialities of this technique in bringing out the finest details in the spectra are well illustrated in his paper. His (Schröter 1965a) figure 6 shows that the displacement is small in the line core, and the asymmetry reaches a maximum value at a distance of 0.8 times the radius of the spot from the spot centre. The centre to limb variations of the Evershed velocities at a fixed location from the centre of the spot shows that the velocities increase towards the limb reaching a maximum at $\mu \approx 0.4$. He also studied the variation of the asymmetry using the line Fe I 5123 Å within the penumbra. The core of the line shows small displacements which increases away from the core and again falls less steeply at the wings. According to him, the sunspot spectra obtained at high spatial resolution show not only line asymmetry but resolve into strong satellites (as seen by Bumba), which appears diffuse at the photosphere - penumbra boundary and rather sharp on the other side of the line centre.

The Evershed flow in the photosphere - chromosphere interface region was investigated by Bones and Maltby (1978) from the velocities in the core and in the wings of the Mg b_1 line using high resolution spectra. The measured velocities (~ 1.8 km/sec) follow the pattern already known from earlier studies. Another front from which the motions in sunspots were investigated was by using high spatial resolution photographs of sunspots. From the time sequence photographs of the Princeton stratoscope project Schröter (1962) was able to detect the systematic motions of the bright knots in the bright penumbral filaments. These knots which form part of the filaments move outward from the centre of the spot with a mean velocity of ~ 2km $\sec^{-1}$. He also detected material motion in the opposite direction in the dark channels that lie in between the bright filaments. There could be little doubt that these proper motions of the bright knots represent the Evershed flow that we see in the spectra of spots. Some of Bhatnagar's spectra (1964) show continuum brightness fluctuations in the penumbral regions that represent the motions of the bright knots. Maltby's (1975) results on the velocities in the chromosphere derived from H_α filtergrams obtained on either wings at $\Delta\lambda \pm 0.25$ Å, ± 0.5 Å and ± 0.75 Å with a resolution of 1/8 A provide a three dimensional picture of the Evershed flow and its variation with time. The flow which is concentrated in channels is directed towards the umbra. These velocity channels occur mostly in regions occupied by the dark fibrils, whereas the flow channels with velocity directed away from the spot appear bright as in the continuum (Schröter, 1962). One interesting point is that the apparent length of the flow channels differ at different heights - they are long in the chromosphere (~ 16 arc sec) and shorter at the lower levels (~ 7 arc sec). The flow channels which are in the form of loops alter with a characteristic time of about 10 minutes which possibly also represents the characteristic time of perturbations of the flow channels.

Finally, I shall mention about the high spatial resolution two dimensional observations of Sheeley and Bhatnagar (1971) and of Sheeley (1972) which have provided a final answer to some of the questions relating to the Evershed flow. For example the question where the Evershed flow terminates has been a subject of much dispute since the time of its discovery. They derived a series of Dopplergrams from a time lapse sequence of spectroheliograms obtained on either wings of the Zeeman insensitive line Fe I 5434 A. These velocity field pictures showed clearly that the Evershed flow confines itself to the dark spoke like filaments that end in the rugged outer boundary of the penumbra and the magnitude of the Evershed velocity is ~ 4-6 km $\sec^{-1}$. Besides this, they also noticed an extra penumbral horizontal flow with speeds of 0.5 - 1.0 km $\sec^{-1}$ which extended to 10,000 - 20,000 km beyond the penumbral boundary. Comparison of these Dopplergrams with the CN 3883 Å spectroheliograms showed that this extra penumbral flow terminated at the facular network. This high spatial resolution study established that the extra penumbral flow is indistinguishable from the well known supergranular flow and is distinctly different from the Evershed flow.

In conclusion I shall list the salient points which require immediate attention and study.

I. The relation between the Evershed velocities and the size of the spot and the magnetic field configuration associated with it should be firmly established.

II. We do not know how the motions are related to the evolutionary aspects of the spots? At what phase of the growth of the sunspots does the flow start? How are velocities related to the age of the spot?

III. The problem of tangential velocities should be settled.

IV. According to Galloway's model of the Evershed flow, the flow is in the form of pulses. It would be interesting to check for any periodicities or the pulse nature of the flow.

V. How are the line asymmetries caused?

VI. What is the nature of the velocity pattern in bipolar spots?

Answers to these questions from studies at high spatial and spectral resolution should help us to understand fully the macroscopic structure of the Evershed phenomenon which even to this day remains as enigmatic as it was 75 years ago.

References

Abetti, G., 1932, Mem. Soc. Astr. Ital. **6**, 353.

Bhatnagar, A., 1964, Ph.D. Thesis, Kodaikanal, Unpublished.

Bones, J., and Maltby, P., 1978, Solar Phys. **57**, 65.

Brekke, K., and Maltby, P., 1963, Ann. Astrophys. **26**, 383.

Bumba, V., 1960, Izv. Krym. Astrofiz. Obs. **23**, 253.

Bumba, V., 1963, Bull. Astron. Inst. Czech. **14**, 137.

Evershed, J., 1909a, Mon. Not. Roy. Astron. Soc. **69**, 454.

Evershed, J., 1909b, Kodaikanal Obs. Bull. **2**, No.15, 63.

Evershed, J., 1909c, Mem. Kodaikanal Obs. **1**, Part I.

Evershed, J., 1910, Mon. Not. Roy. Astron. Soc. **70**, 217.

Evershed, J., 1916, Kodaikanal Obs. Bull. **3**, No.51, 167.

Hale, G.E., 1908, Astrophys. J. **28**, 314.

Holmes, J., 1961, Mon. Not. Roy. Astron. Soc. **122**, 301.

Holmes, J., 1963, Mon. Not. Roy. Astron. Soc. **126**, 155.

Kinman, T.D., 1952, Mon. Not. Roy. Astron. Soc. **112**, 425.

Kinman, T.D., 1953, Mon. Not. Roy. Astron. Soc. **113**, 613.

Maltby, P., 1964, Astrophys. Norveg, **8**, 205.

Maltby, P., 1975, Solar Phys. **43**, 91.

McMath, R.R., Mohler, O.C., Pierce, A.K., and Goldberg, L., 1956, Astrophys. J. **124**, 1.

Michard, R., 1951, Ann. Astrophys. **14**, 101.

Schröter, E.H., 1962, Z. Astrophys. **56**, 183.

Schröter, E.H., 1965a, z. Astrophys. **62**, 228.

Schröter, E.H., 1965b, Z. Astrophys. 62, 256.

Schröter, E.H., 1967 In Solar Physics, ed. John N. Xanthakis; Interscience Pub. p.325.

Servajean, R., 1961, Ann. Astrophys. **24**, 1.

Sheeley, N.R., and Bhatnagar, A., 1971, Solar Phys. **19**, 338.

Sheeley, N.R., 1972, Solar Phys. **25**, 98.

St. John, C.E., 1913, Astrophys. J. **37**, 322.

DISCUSSION:

GOKHALE: Has anyone looked for short time scale variations in Evershed velocity?

SIVARAMAN: In the model of Galloway he shows that Evershed phenomenon is in the form of pulses. It would be worthwhile to obtain time lapse spectra and search for any temporal periodicities.

Kodaikanal Obs. Bull. (1984) 4, 19-24.

CONVECTION AND THE PHENOMENON OF KILOGAUSS MAGNETIC FIELDS ON THE SUN

P. Venkatakrishnan
Indian Institute of Astrophysics
Bangalore 560034
INDIA

Abstract

The role played by convection in the formation of slender magnetic flux tubes and in the dynamics of the gas within the tube is discussed in the case of simplified models. Convection instability cannot drive systematic downflows whereas convective buffeting of the tube can. The inclusion of heat transport reduces the efficiency of convective collapse for the formation of strong fields. The implications of these two results for the solar magnetic flux tubes is pointed out.

1. Introduction

The interaction of velocity and magnetic fields has been well studied in the context of magnetoconvection. The work of Parker (1963), Weiss (1966), Proctor and Galloway (1979), Galloway and Weiss (1981), all indicate that in a Boussinesq fluid the final result of the interaction of a circulatory velocity field and a uniform magnetic field is the formation of a structured magnetic field devoid of flow and a region of flow bereft of magnetic field. It is natural to ask the question whether such structures can be formed even in the case of compressible magnetoconvection. This question is particularly important in the light of the highly structured nature of the magnetic fields observed on the solar surface.

One way of answering this question would be to assume a family of equilibrium structures and examine their stability as a function of some parameter characterising the family, e.g. the magnetic field. Stability analysis of two dimensional structures (e.g. an axisymmetric tube with area of cross-section varying with height) is exceedingly difficult. The slender flux tube approximation, introduced conceptually by Defouw (1976) and established rigorously by Roberts and Webb (1978), helped in the linear stability analysis of such structures. Webb and Roberts (1978) showed that tubes with field strengths smaller than a critical value are prone to a convective instability. The critical value depends on the depth of the tube as well as on the superadiabatic temperature gradient. Spruit and Zweibel (1979) calculated the growth rates of the instability for tubes embedded in a realistic convection zone environment. Their critical field strength was ≈ 1500 G. These values compare well with the observed field strengths.

However, one does not know a priori whether the convective collapse of weaker tubes would result in a hydrostatic tube or hydrodynamic tube within the time scales of interest in the solar context. Hasan (1983) calculated the nonlinear development of convective instability of a slender flux tube and obtained final hydrodynamic states independent of the initial value of the magnetic field. In this paper we review some of our results of similar calculations for polytropic tubes, both for adiabatic (Venkatakrishnan, 1983) as well as non-adiabaic (Venkatakrishnan, 1984a) conditions.

Furthermore, the magnetic structures observed in the photosphere are constantly buffetted by granulation and waves. We shall also consider the nonlinear response of magnetic tubes to such perturbations.

2. Nonlinear Development of Convective Instability with Slender Flux Tubes

The various parameters that determine the evolution of a polytropically stratified slender flux tube are β_0, the ratio of initial gas pressure of magnetic pressure, δ_0 the initial superdiabatic gradient and the boundary conditions. The basic equations for a slender flux tube were first rigorously formulated by Roberts and Webb (1978). These equations are:

$$\frac{\partial}{\partial t}(\rho/B) + \frac{\partial}{\partial z}(\rho v/B) = 0, \qquad (2.1)$$

$$\frac{\partial v}{\partial t} + v\frac{\partial}{\partial z}v + \frac{1}{\rho}\frac{\partial}{\partial z}p + g = 0 \qquad (2.2)$$

$$\left(\frac{\partial}{\partial t} + v\frac{\partial}{\partial z}\right)p - \frac{\gamma p}{\rho}\left(\frac{\partial}{\partial t} + v\frac{\partial}{\partial z}\right)\rho = -(\gamma-1)\,(\nabla.\underset{\sim}{F}) \qquad (2.3)$$

$$B^2 = 8\pi\,(p_e - p), \qquad (2.4)$$

where p, ρ, v, B are the pressure, density velocity and magnetic field inside the tube, p_e is the pressure outside the tube and $\underset{\sim}{F}$ is the energy flux. We shall first consider the case $\underset{\sim}{F} = 0$ corresponding to adiabatic motions.

2.1. Adiabatic Flow

The equations (2.1) through (2.4) with $\underset{\sim}{F} = 0$ form a system of hyperbolic partial differential equations which can be cast in the characteristic form. We integrated these equations using a backward marching algorithm based on the method of characteristics (For details see Venkatakrishnan, 1984b). In this way we obtained the values of all the dynamical variables as a function of z for various instants of time. In this paper we shall mainly discuss the evolution of velocity and magnetic field of the tube at a few spatial locations.

We applied two different sets of boundary conditions. In one set the Eulerian pressure was kept constant at both ends of the tube. These conditions could be more appropriate to closed magnetic regions of the sun (Venkatakrishnan, 1983). The tubes on which such conditions were applied will be called 'closed' tubes in what follows. In the other set of boundary conditions the Eulerian pressure was kept constant at the base of the tube while the Lagrangian pressure was kept constant at the top of the tube. This type of boundary conditions would be more appropriate for open vertical tubes in the sun. These tubes will be denoted as 'open' tubes in what follows.

The general behaviour of velocity for the adiabatic case consisted of an initial slow increase till a time τ and then a rapid increase beyond that time. The onset of the nonlinear phase was delayed for stronger initial magnetic fields (small values of β_0). It was apparent that $\tau \to \infty$ as β_0 tended to some finite value ≈2.0 (Figure 4 of Venkatakrishnan, 1983). Furthermore, the intensification of the field was not seen to be sustained during the nonlinear phase for β_0 = 4.0, 5.0 and 6.0. An interesting example of overstability was seen for β_0 = 2.0 in the case of an open tube. When β_0 = 4.0, however, it was seen that steady magnetohydrodynamic states are attained. For β_0 = 6.0, the nonlinear regime showed unsteady behaviour even until 30 free fall times.

The following picture emerged out of these calculations. The magnetic field inhibits the convective collapse of flux tubes. For some value of the field, overstable oscillations set in while for weaker fields steady dynamic states are attained. Even this is not possible for the weakest fields studied here, and in these cases unsteady behaviour persists for large times. The actual values of field strengths demarcating these regimes depends on the boundary conditions, with open tubes exhibiting greater stability compared to closed tubes.

2.2. Effect of Radiative Heat Transport

The energy equation for an optically thick slender flux tube is:

$$\left(\frac{\partial}{\partial t}+v\frac{\partial}{\partial z}\right)p-\left(\frac{\gamma p}{\rho}\right)\quad\left(\frac{\partial}{\partial t}+v\,\frac{\partial}{\partial z}\right)\rho\;=(\gamma-1)K$$

$$\left[\left\{\frac{4(Te-T)}{r_0^2}+\frac{\partial^2T}{\partial Z^2}\right\}+\left(\frac{\partial T}{\partial z}\right)^2\left(\frac{\partial}{\partial T}+\frac{\partial p}{\partial T}\frac{\partial}{\partial p}\right)\ \ln K\right].\quad(2.5)$$

(For a derivation of this equation see Venkatakrishnan 1984a). The first term on the R.H.S. of the equation (2.5) represents the lateral heat exchange. The second term represents longitudinal heat diffusion for constant heat conductivity K, while the third term represents the influence of variable conductivity. Here we shall discuss only the case of constant K.

When lateral heat exchange alone was considered in an open tube, it was seen that oscillations were produced. The amplitude of these oscillations increased with decreasing radius r_0 of the tube. For r_0 < 0.5 the oscillations became so large that local pressure enhancements rendered the magnetic field imaginary and precluded further computations. The amplitude of oscillation was seen to be drastically reduced for β_0 = 4.0, as compared to the case for β_0 = 6.0. When longitudinal heat transport was included, the frequency of the oscillations was seen to be doubled and the amplitude reduced. This perhaps could be due to the excitation of a new mode or harmonic.

Thus heat transport was seen to shift the state of marginal stability to lower values of the magnetic field as compared to the adiabatic case. Wherever the instability was evidenced, it was only in the form of oscillations and not monotonic as seen in the case of adiabatic flow.

3. Response of Tubes to External Turbulence

Let us for a moment forget the considerations of stability and assume that a stable magnetostatic flux tube exists in the solar atmosphere. This tube cannot remain static since it is embedded in a highly chaotic environment. The environment can influence the tube broadly in 3 ways. It can twist, bend or squeeze the tube. A twist cannot influence the dynamics of the gas inside the tube while bending and squeezing motions can. In what follows we report some results concerning the response of this gas to bending motions of the tube (Hasan and Venkatakrishnan 1980) as well the response to squeezing motions (Venkatakrishnan, 1984b).

3.1. Response of Squeezing Motions

The equations (2.1) through (2.4) described the state of a tube with a time independent environment. If external pressure perturbations are applied then they would induce changes in the internal gas pressure and, therefore, create a flow of gas along the field. We applied two forms of external perturbations. In one form the fluctuations were oscillatory in time but decreasing exponentially with height. The response of the gas within the tube is maximum when the scale length of the perturbation is approximately equal to the distance travelled by a tube wave in one period of the oscillation (Figure 1). Moreover, the resulting flow along the tube is oscillatory. When the scale length is smaller than the tube travel length, the velocity amplitude is smaller and the flow tends to drift into a down flow.

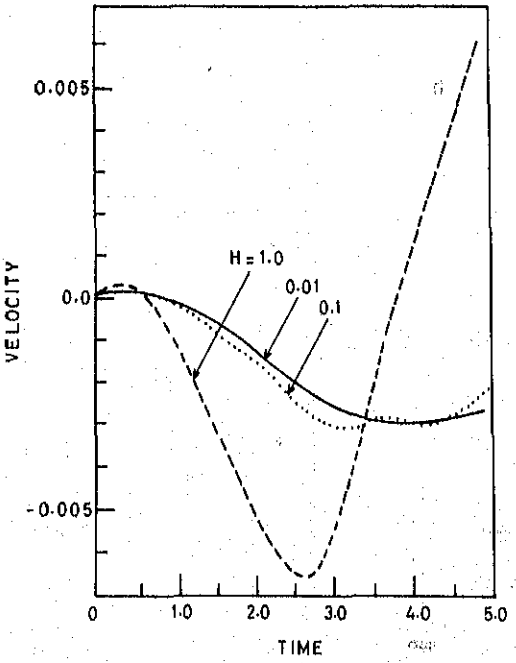

Fig.1. Response of gas to squeezing motions on the tube - effect of exponentially decaying fluctuations with different values of scale height H.

The second form of the pressure perturbation was chosen to be oscillatory in space as well as in time. In this case, the maximum response is seen to occur when the wavelength of the perturbation matches with the tube travel length (Figure 2). This confirms the resonance predicted by Roberts (1979) on the basis of linear analysis. It must be seen, however, whether the resonant build up of amplitudes leads to a shock wave or whether the resonance is destroyed at large times.

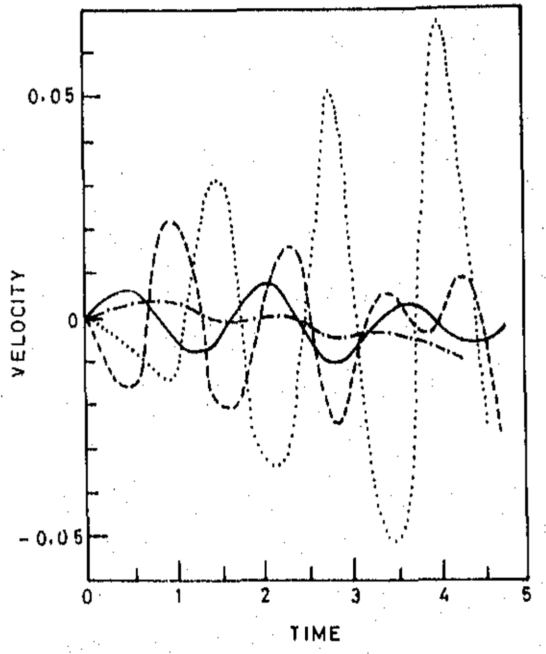

Fig.2. Same as in Figure 1 but for wavelike pressure fluctuations for various ratios λ of wave to tube speed.

For the solar atmosphere if one takes the dimensions of the scale height of granular velocity decay into account then it would seem from these results that for strong tubes the most preferred response would be an oscillatory flow.

3.2. Response to Bending Motions

In order to study bending motions,

it is convenient to consider the motion of infinitesimal flux tubes with area of cross-section δA which is inversely proportional to the local field strength. For this case, we imposed a lateral velocity for the field line and studied the resulting flow along the field. The equations relevant to this study were written in a frame of reference moving with the field line. These euations are (Hasan and Venkatakrishnan, 1980):

$$\frac{dV_s}{dt} + V_s \frac{dV_s}{ds} = -\frac{1}{\rho}\frac{dp}{ds} - g\cos\theta + V_n \frac{d\theta}{dt} + V_n V_s \frac{d\theta}{ds}, \qquad (3.1)$$

$$\frac{d\ln\rho}{dt} + V_s \frac{d\ln\rho}{ds} + \frac{dV_s}{ds} = -V_s \frac{\partial\theta}{\partial n} + V_n \frac{d\theta}{ds} - \frac{\partial V_n}{\partial n}, \qquad (3.2)$$

$$p/\rho^{\Gamma} = \text{constant}, \qquad (3.3)$$

where p, ρ, V_s and θ are the gas pressure, density, velocity along the field, and the angle made by the field to the vertical respectively. The coordinate 's' is the distance measured along the field and V_n is the velocity normal to the field direction. Once again these equations were integrated by the method of characteristics. A detailed description of the resulting motion for two assumed forms of V_n is given in Hasan and Venkatakrishnan (1980). The main result is that gas is seen to be accelerated in the direction of increasing V_n. Physically this effect is because of the centrifugal acceleration on the gas constrained to move in a curved path because of the non-uniform V_n.

This effect can be applied to the case of granule flux tube interaction. It is known that the rms granular velocity decreases with height (Durrant et al. 1979). Thus if the tube is bent with a corresponding lateral velocity decreasing with height, then a downflow would result. A numerical simulation of this effect was performed by Venkatakrishnan and Hasan (1981). The resulting velocities (Figure 3) compared favourably with some observations (e.g. those of Giovanelli et. al. 1978). A detailed account of the limitations of such an approach of modelling the interaction can be found in Venkatakrishnan (1984b).

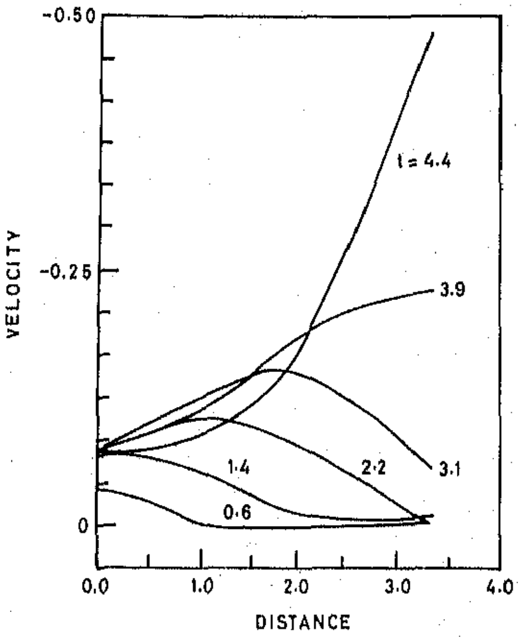

Fig.3. Interaction of granules with magnetic flux tubes - evolution of spatial velocity profiles.

4. Application to Solar Kilogauss Fields

There are two ways in which one can consider these results in the context of the tiny kilogauss flux tubes found in the solar photosphere. If one considers the dynamics of the gas within these flux tubes, then it would appear from all the above results that convective collapse with heat transport and external pressure fluctuations both produce only oscillatory motion. It is only the buffetting of granules that can be expected to drive the observed downflows in these tubes. The problem of gas supply exists, however, and there is a school of thought which even doubts the reality of the downflows. However, the fact remains that the stochastic jostling of flux tubes with a spatially stationary gradient in the rms amplitude would necessarily lead to a downflow. The question only remains as to the exact magnitude of the downflow. Recent observations using the 1-m FTS at Kitt Peak National Observatory (Stenflo et al. 1984) do demonstrate the necessity of including velocity gradients in flux tube models.

The second aspect concerns the problem of convective collapse. For polytropic tubes we have shown that radiative heat diffusion shifts the state of marginal stability to lower values of the field and introduces oscillations of the field strength as well. It remains to be seen whether calculations for non-polytropic realistic tubes would yield similar results. Such calculations would put better theoretical limits on the minimum field strength of the flux tubes and also provide the exact amplitudes and periods of the oscillations, if any.

References

Defouw, R.J., 1976, Astrophys. J. **209**, 266.

Durrant, C.J., Mattig, W., Nesis, A., Reiss, G. and Schmidt, W., 1979, Solar Phys. **61**, 251.

Galloway, D.J., and Weiss, N.O., 1981, Astrophys. J. **243**, 945.

Giovanelli, R.G., Livingston, W.C., and Harvey, J., 1978, Solar Phys. **59**, 49.

Hasan, S.S., 1983, IAU Symp. No.102, 73.

Hasan, S.S., and Venkatakrishnan, P., 1980, Kodaikanal Obs. Bull. Ser.A., 3, 6.

Parker, E.N., 1963, Astrophys. J. **138**, 552.

Proctor, M.R.E., and Galloway, D.J., 1979, J. Fluid Mech. **90**, 273.

Roberts, B., 1979, Solar Phys. **61**, 23.

Roberts, B., and Webb, A.R., 1978, Solar Phys. **56**, 5.

Spruit, H.C., and Zweibel, E.G., 1979, Solar Phys. **62**, 15.

Stenflo, J.O., Harvey, J.W, Brault, J.W., and Solanki, S., 1984, Astron. Astrophys. **131**, 333.

Venkatakrishnan, P., 1983, J. Astrophys. Astron. **4**, 135.

Venkatakrishnan, P., 1984a, J. Astrophys. Astron. (In press).

Venkatakrishnan, P., 1984b, Ph.D. Thesis, Bangalore University.

Venkatakrishnan, P., and Hasan, S.S., 1981, J. Astrophys. Astron. **2**, 133.

Webb, A.R., and Roberts, B., 1978, Solar Phys. **59**, 249.

Weiss, N.O., 1966, Proc. Roy. Soc. London, Ser.A., **293**, 310.

DISCUSSION:

BALASUBRAMANIAM: What sort of observations can one make, to look for these oscillations in sunspots? How do you think they will show up?

VENKATAKRISHNAN: Oscillations are already known to occur in sunspots. My work is aimed at tiny flux tubes. Only observations of high spatial resolution can detect the oscillations of field strength. Velocity oscillations can be detected using the shift in the zero point of the V-Stokes profile but one needs high spectral resolution in this case.

GOPALSWAMY: Can your computations be used for some inferences regarding the three tier nature of solar convection zone? For example, in the middle convection tier a single strong flux tube gives rise to many thin flux tubes in the upper tier, where the radiation becomes very important. Can the oscillation of the middle tier flux tubes be considered as the temporal shaking of the thin upper tier flux tubes?

VENKATAKRISHNAN: One can always think of a scenario where the hierarchy of magnetic structures is governed by the hierarchy of convective cells. However this is beyond the scope of my work. Moreover my work is concerned with the dynamics of individual tubes and can therefore say nothing regarding aggregates of tubes coupled to each other.

Kodaikanal Obs. Bull. (1984) 4, 25-34.

SOLAR DYNAMO PROBLEM

M.H. Gokhale
Indian Institute of Astrophysics
Bangalore 560034
INDIA

Abstract

The origin of solar magnetic field and the flux tube nature of this field on the smallest observed scales are two key problems in solar magnetohydrodynamics. Despite the success of kinematical models based on the turbulent dynamo theory, continuation of thinking on alternative approaches is justified and may be even necessary.

One such approach is based on consideration of energy transfer in magnetogasdynamical production of new magnetic fields near the base of the solar convection zone. It turns out that the field produced by a substantial transfer of energy from the flows will essentially be in the form of strong thin flux sheaths that may break into 'cluster of flux tubes' similar to those observed on the sun. Quantitative similarity requires nonlinear MHD interactions of flows with amplitudes $\sim 10^4$ cm s^{-1} on timescales $\sim 10^3$s. Such interactions may be provided by azimuthal magnetoacoustic waves at the longitudes where they cross one another. The required wave amplitudes can be provided by a small fraction of the outward energy flux which must be blocked near the base of the convection zone. The resulting phenomenological model of the magnetic cycle provides for (i) two varieties of activity with distributions and phases similar to the XBP and sunspot cycle, (ii) poleward migrations of large scale fields, (iii) long lived coronal hole like magnetic structures during decline of the sunspot cycle and (iv) relations between the decline of each cycle and the amplitude of the succeeding cycle. The basic postulate of this model remains to be established from solutions of MHD equations. However if established, it will provide promising alternative to the turbulent dynamo model.

1. Introduction

Solar magnetohydrodynamics can be said to have begun with the discoveries of strong magnetic fields and Evershed flows in sunspots. The present scope of the solar MHD covers various problems concerning the following phenomena (e.g. Priest 1982): (i) sunspots, (ii) quiescent prominences, (iii) transient events like flares, active prominences and coronal transients, (iv) coronal heating and coronal structures, (v) solar wind and interplanetary magnetic field, (vi) solar dynamo and solar activity cycle and (vii) the small scale magnetic flux tubes in the photosphere and chromosphere. The boundary conditions used in modelling of the first five phenomena are often based on an ad-hoc choice of photosphere (or some other surface like the Alfvénic surface) as one of the boundaries. Secondly the often observed inhomogeneities and discontinuities in directions transverse to the field are ignored in most of the models of these phenomena. The progress in the modelling of these phenomena will depend ultimately on the boundary conditions at the "innermost boundaries" of the magnetic structures (i.e. the depths at which the field lines originate) and also upon the physical conditions and processes in the individual flux tubes constituting the magnetic structures.

Thus, the solar dynamo problem and the problem of thin magnetic flux tubes can be considered as two key problems in the solar magnetohydrodynamics.

In this review, I shall briefly discuss the various approaches to the solar dynamo problem and present a somewhat detailed discussion of a new phenomenological approach which will bring out a likely connection between dynamo problem and the problem of thin flux tubes.

2. Behaviour of the Solar Magnetic Field on Different Length Scales and Time Scales

Because of its key role in almost the whole of the solar MHD, a model of the solar dynamo should be ultimately consistent with the behaviour of solar magnetic field as observed (or observationally inferred) on different length scales and time scales. I have listed in Appendix I as many observed properties of the solar magnetic field as known from different observations which are relevant to the present discussion. The purpose of presenting this list is not to suggest any attempt to "explain" all these phenomena with a single theory. It is only to illustrate how vast is the amount of observational information that a solar dynamo theory will have ultimately to deal with.

3. Solar Dynamo Problem as the Solar Cycle Dynamo Problem

Solar magnetic fields would not have posed any dynamo problem if the observed large-scale field could be understood as a manifestation of the remnant of a 'primordial field' which must have been trapped in the sun during its formation. Theoretically, the presence of such a fossil field cannot be ruled out even though the sun must have gone through a fully convective state in the past (Piddington, 1982). However, such a fossil field, if present, seems to be too weak to be detected in the noise of the strong fields associated with the solar cycle whose surface average near polar region does reverse every 11 y or so. Thus, the solar dynamo problem is essentially that of the dynamo which provides the fields that manifest as the solar cycle.

4. Different Approaches to Theoretical Modelling of the Phenomenon

A theoretical model of any phenomenon must ultimately satisfy the following primary and auxiliary criteria:

C_1: Consistency with the basic laws of physics (primary),

C_2: Consistency with the relevant well established observations (primary), and

C_3: Consistency with well established theories of other related phenomena (auxiliary).

Depending upon the initial emphasis on C_1 or C_2, three kinds of alternative approaches are possible.

Physical: (Initial emphasis on C_1) - Zero order model is constructed by solving as many equations representing relevant laws of physics as possible.

Semi-phenomenological: (Mixed initial emphasis) - Zero order model is constructed by solving some simpler sub-set of basic equations and replacing other equations by plausible postulates which provide consistency with some important observations.

Phenomenological: (Initial emphasis on C_2)
- Zero order model is itself a minimal set of plausible and mutually consistent postulates having "provisions for consistency" with as many observations as possible.

5. Successes and Failures of Existing Solar Dynamo Models Based on Such Approaches

The following solar cycle dynamo models have so far been attempted from the above approaches:

Phenomenological:

Babcock's model (1961), Piddington's (1971) model.

Semi-phenomenological:

i) Oscillator models: (e.g. Layzer et al. 1979). In these, the equations of continuity, momentum, magnetic non-divergence are solved whereas the energy equation is ignored.

ii) Turbulent dynamo models: (e.g. Parker, 1963; Stix, 1976; Yoshimura, 1979; Krause and Radler, 1980). In these only the equations of magnetic induction and non-divergence are solved whereas equations for continuity, momentum and energy are replaced by assumptions about the convective flows and turbulence.

Physical:

(Gilman and Miller, 1981). All essential MHD equations are solved, except that effects of turbulence are parametrized.

Naturally, the physical models have the least a-priori 'provision for consistency' with the observed behaviour of the solar magnetic field and plasma motions on different scales. However, the importance of these models lies in showing how difficult it is to satisfy both the criteria, C_1 and C_2, and how far away the present modelling atempts are from the ultimate goal of a satisfactory model. The relaxation of criterion C_1 (ignoring the energy equation) in oscillator models has not yielded commensurate success in satisfying the criterion C_2 (cf. Cowling, 1981). The turbulent dynamo models, which further ignore the momentum equation also, are relatively much more successful. Unfortunately, the turbulent dynamo models are open to several doubts and difficulties (e.g. Piddington, 1981; Cowling, 1981) which are summarized in Appendix II.

In the solar dynamo problem, the phenomenological approach is most suitable since the abundance of observational information might be used to identify and isolate most pertinent physical questions for further investigation. Thus, Babcock's model did provide for qualitative agreement with most of the then known behaviour of the solar magnetic fields on length scales $\lesssim R_\odot$ and timescales $\sim 11y$ (e.g. the polarity and orientation laws of bipolar regions, migrations of fields and butterfly diagrams). One great drawback of the model, however, was that the evolution of three dimensional topology of its magnetic fields - as required to account for the reversal of the global poloidal field was extremely unsatisfactory. In the framework of its own phenomenology, the magnetic buoyancy invoked to bring the toroidal flux ropes to the surface would more probably remove all the magnetic flux from the sun (e.g. Piddington, 1972).

6. An Alternative Phenomenological Approach

An alternative phenomenological approach which I have developed since last several years (Gokhale, 1977, 1979a,b) is intended to retain the advantages of Babcock's model and to eliminate the difficult situation that the magnetic buoyancy might eventually remove all the magnetic flux from the sun. This difficulty will be remedied if some MHD process keeps producing new magnetic flux in the sun on timescales $\lesssim 11$ y, at an average rate needed to balance the loss due to magnetic buoyancy.

6.1. The Timescale of the Most Efficienct MHD Generation of New Magnetic Flux

Magnetohydrodynamical generation of a new magnetic flux implies transfer of energy from the plasma flow to the electromagnetic field at a rate exceeding the ohmic dissipation.

For a flow of velocity $\underline{u}$ transverse to a magnetic field of intensity B_0 the timescale τ of such an energy transfer must satisfy

$$[\rho]\,[u^2]\,[\tau]^{-1} \gtrsim [\sigma]\,[u^2]\,[B^2]$$

i.e.

$$[\tau]^{-1} \gtrsim [\sigma]\,[B^2]\,[\rho]^{-1},$$

where square brackets denote the orders of magnitudes of the bracketed quantities, σ is the electrical conductivity and ρ the density at the place of interaction. It is assumed here that there is no external electric field, so that the mean current density is $\sim \sigma u B_0$. The most efficient energy transfer would imply conversion of a substantial fraction of the flow energy and hence the corresponding timescale will be given by

$$[\rho]\,[u^2]\,[\tau]^{-1} \approx [\sigma]\,[u^2]\,[B_0^2]$$

i.e.

$$[\tau] \approx [\sigma]^{-1}\,[B_0]^{-2}\,[\rho] \qquad (1)$$

6.2. Generation of Magnetic Flux Sheaths and the Resulting Clusters of Strong, Thin Flux Tubes

For conditions near the base of the convection zone ($\sigma \approx 10^5$ emu, $B_0 \approx 3$ G and $\rho \approx 10^{-1}$ gm cm^{-3}), equation (1) implies:

$$\tau \approx 10^3 \text{ s}$$

For velocities $u \approx 10^4 - 10^5$ cm s^{-1} (comparable to the velocity of solar rotation), the mean field intensity B_* in the resulting electromagnetic structure will be $\approx 10^4 - 10^5$G and the thickness of the structure will be as small as $\approx 10^7$-10^8 cm. The other two dimensions of the structure will be comparable to the corresponding dimensions of the flow, which will be generally $\gg \delta$. Hence, the newly generated structures will consist of electric current sheaths and associated magnetic flux sheaths. If the dimensions H, $\perp$ to both $\underline{u}$ and $\underline{B}_0$ is $\approx 10^{10}$ cm (density scale height near the base of the convection zone), then the total flux in each magnetic flux sheath will be

$$\Phi \approx B_* H \delta \approx 10^{21}\text{-}10^{23} \text{ Mx}$$

Each such magnetic flux sheath may be expected to 'crumple' sooner or later, into a 'cluster of flux tubes'. The amount of magnetic flux ϕ in an individual flux tube will be

$$\phi \approx B_* \delta^2 \approx 10^{18}\text{-}10^{21} \text{ Mx}$$

It is quite interesting to note that for $\underline{u} \approx 10^4$ cm s^{-1} the cluster will have a total magnetic flux $\Phi \approx 10^{21}$ Mx, which is comparable to the flux in a typical sunspot group, and each flux tube in the cluster will have a flux $\phi \approx 10^{18}$ Mx which is comparable to the flux in most of the individual flux tubes observed on the photosphere.

6.3. What kind of MHD flows can attain velocities $\approx 10^4$ cm s^{-1} near the base of of the convection zone?

From energy flux considerations alone, velocities $\sim 10^4$ cm s^{-1} cannot be ruled out for convective flows near the base of the convection zone. However, the corresponding mass flux will imply too high velocities ($\sim 10^7$ cm s^{-1}) near the surface, which are never observed. Hence, convective flows may not have velocities $\sim 10^4$ cm s^{-1} near the base of the convection zone, unless their mass circulation is somehow closed much below the observable layers, which is rather unlikely.

Let us, therefore, consider oscillatory flows like those associated with waves. Out of the three types of waves with $\underline{U} \perp \underline{B}_0$, the slow and Alfvén modes are too slow to yield energy transfer on timescales $\sim 10^3$ s. On the other hand, the fast (i.e. magnetoacoustic modes with wavelength $\sim R_\odot$ do have timescales $\sim 10^3$ s. Among such modes the radially propagating modes cannot have amplitude $\sim 10^4$ cm s^{-1} near the base of the convection zone, since the corresponding radial energy flux would be four orders of magnitudes larger than the total energy flux at the surface. Since the background field is poloidal, the only remaining kind of magnetoacoustic mode $\underline{U} \perp \underline{B}_0$ are the azimuthal ones, and there seems no reason why these cannot attain amplitudes $\sim 10^4$ cm s^{-1}.

6.4. Mechanism for Energizing the Magneto-acoustic Modes Near the Base of the Convection Zone

Near the base of the convection zone, there will be a layer of finite thickness where the temperature gradient is superadiabatic but the superadiabaticity is below the critical value required for large-scale convective instability. In such a layer, the minute fraction of the outward energy flux which cannot be carried further either by radiation or by convection will be "blocked". This blocked flux must go in energizing various waves including the azimuthal magnetoacoustic waves.

6.5. Amount of Energy Required for Wave Amplification Upto 10^4 cm s^{-1}

For building up wave amplitudes $\approx 10^4$ cm s^{-1} the required average value of the blocked energy flux will be only $\sim 10^8$ erg cm^{-2} s^{-1} i.e. only ≈ 0.1 - 1% of the total radial energy flux (also comparable to the mean value of the non-radiative flux deposited above the photosphere).

6.6. Locations of Interactions

Conservation of angular momentum requires that the azimuthal MHD modes be generated in pairs of oppositely propagating waves which keep on repeatedly crossing each other at a finite number of longitudes, where the steepest gradients of velocity and magnetic fields would develop. Therefore, it is in the neighbourhood of such longitudes that the non-linear interactions satisfying equation (1) may be localized.

6.7. A Tentative Postulate

On the basis of the foregoing discussion we arrive at the following tentative phenomenological postulate:

Near the base of the convection zone a minute fraction of the outgoing energy generates and amplifies oppositely propagating azimuthal magnetoacoustic waves and these waves produce strong, then, electric current sheaths and magnetic flux sheaths through nonlinear interactions near the meridians where they cross one another. The foregoing postulate remains to be verified by detailed magnetogasdynamical calculations. However, let us assume its validity for the present and proceed to see how one could develop from it a phenomenological model with provisions for agreement with several important observed characteristics of the solar cycle.

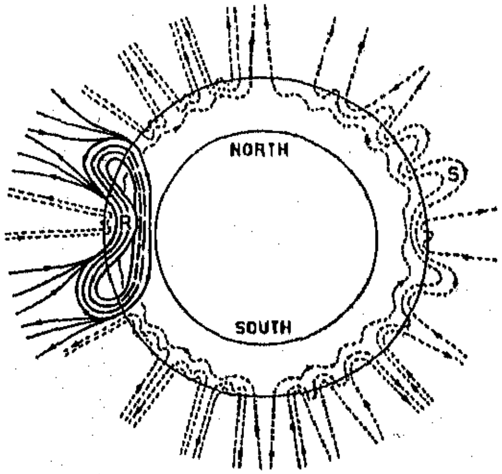

Fig.1. A schematic diagram of the phenomenological model. Thick lines represent one of the several newly created magnetic "flux rolls". Thin lines represent the background magnetic field "S". This background field (S) and the front portions (R) of the newly created "Flux rolls" emerge above the photosphere providing two varieties of activity with similar polarities but differing in phase, surface distribution and magnetic flux per active region. Meanwhile the back portions of the flux rolls, represented by dashed lines, diffuse over all latitudes and longitudes to provide the reversed background field for the next cycle.

For convenience of illustration only one newly created flux roll is shown, and no attempt is made to show effects of differential rotation.

6.8. Consequences

6.8.1. Reversal of the Global Field

The newly produced magnetic structures must necessarily be topologically closed. Thus the flux sheaths must be 'flux rolls' and the flux tubes must be 'flux loops'. Therefore, the reversal of the global field on an 11 y time scale can be achieved if: (i) the background field B_0 and the similarly oriented **front** portions of the newly created flux loops rise upto and above the photosphere gradually on a timescale of 11 y and simultaneously; (ii) the **back** portions of these flux loops diffuse in the base layer to provide a background field $\sim(-B_0)$ for the next cycle (Figure 1).

6.8.2. The Two Varieties of Activity

The global field reversal in the above manner would imply that during any 11 y cycle the activity at and above the photosphere will come from segment-by-segment emergence of the following two varieties of flux tubes (segments from both varieties having similar polarities): (1) The thin, frayed flux tubes of the background field which are present at all latitudes and all longitudes and whose current system and field lines are confined to the outer parts of convection zone and the outer space, and (2) The front portions of the newly produced thick clusters of flux tubes which are present predominently in the central latitudes and neighbourhoods of a few preferred longitudes, and whose current system and field lines are closed near the base of the convection zone. The first variety of segments will, in general, emerge earlier than the latter.

Thus, the model of the field reversa automatically provides two varieties of solar activity with the surface distributions and relative phases similar to the x-ray bright point and sunspot related solar activity. Schüssler (1980) presented a model based on a similar modulation of the thickness of flux tubes responsible for the activity without entering into the question of how the magnetic flux tubes are produced. However, in his model thicker flux tubes rise earlier which seems to contradict the fact that each new cycle starts with appearance of the smallest spot groups (e.g. Gokhale and Sivaraman, 1982).

6.8.3. The Background Magnetic Flux and the Activity Related Magnetic Flux

Since the magnetoacoustic waves of amplitudes $\sim 10^4$ cm s^{-1} are expected to produce magnetic flux rolls of $\sim 10^{21}$ Mx each, the maintenance of the order of magnitude of the background magnetic flux requires that such a production occurs only once during each $\sim$ 11 y or so, (e.g. in association with some catastrophic transformation of the wave) if the azimuthal wave number of the wave is $\lesssim$ 10. In such a case ('catastrophic model') each flux roll will have to emerge in $\sim 10^2$ - 10^3 segments in order to account for the ratio of that order between the activity related flux and the background flux. If the required amplification is provided by the differential rotation as in the Babcock's model, then it will also account for the polarity orientations as in that model.

Alternatively, if the magnetic flux rolls are produced during each wave period ('persistent production model') then the amount in the flux rolls and the rate of their emergence must vary during the 11 y cycle in such a way that the order of magnitude of the background flux is maintained and the number of segments give the right amount of the activity related flux.

These details are yet to be worked out.

6.8.4. Migrations of Large-scale Fields

The emergence of the 'front' portions and the diffusion of the 'back' portions of the newly created fields will lead to poleward migration of the following polarities in the photospheric field along with the neutral lines separating these polarities from the background field (e.g. Howard, 1974; Makarov, et al. 1982; Makarov and Sivaraman, 1983).

6.8.5. Variations of the Sizes and Locations of the Long Lived Coronal Holes and Relations Between the Decline of One Solar Cycle and the Amplitude of the Next Cycle

During the declining years of the sunspot cycle the photospheric intersections of the new magnetic structures will provide deep rooted, monopolar, open field structures at middle latitudes which might account for the occurrence of long lived coronal holes at such latitudes during the declining phase of the solar cycle.

Ultimately, towards the end of the solar cycle, these structures will yield monopolar regions of the reversed polarity near the poles.

6.8.6. The Values of the Period

The period of the solar cycle in such a model will be ultimately determined by the timescale of modulation of the rate of energy trapping near the base of the convection zone. As an illustration it has been shown earlier (Gokhale, 1977) that a value of ~11 y can be obtained (for a 'catastrophic model') by assuming a turbulent viscosity $\sim 10^{11.5}$ cm^2 s^{-1}.

6.8.7. Modulation of the Amplitude of the Cycle

Under 'normal' circumstances a relatively steady cycle may be maintained by an approximate balance among the rates of the following processes: (i) production of magnetic flux near the base of the convection zone, (ii) the rise of flux tubes across the convection zone, (iii) migration and diffusion of magnetic flux across the surface and (iv) the removal of magnetic flux by magnetic buoyancy, reconnections and solar wind. Excursions to and from 'abnormal' conditions like Maunder minima might be caused by some non-linear couplings between these processes.

7. Conclusions

I may conclude by saying that the theory of the solar dynamo is far from the final solution of the problem, although the semi-phenomenological turbulent dynamo models and the fully phenomenological new approach described here continue to be the most promising approaches.

The new phenomenology based on the postulated production of thin electromagnetic structures by locally non-linear interactions of magnetogasdynamical modes provides for agreements with many observed features of the solar cycle on timescales $\lesssim 22$ y. However, it cannot be considered as an established model till the basic postulate is verified by mathematical solution of the relevant magnetogasdynamical equations, and the parameters of the solution are shown to vary on timescales > 22 y in a way consistent with the observationally derived behaviour of the solar cycle on such timescales. The dilemma of catastrophic versus continuous production of new field also needs to be resolved.

Appendix I

OBSERVATIONAL CONSTRAINTS

Magnetic Cycle (Timescales $\lesssim$ 22 y):

1. Reversal of poloidal ($\sim 10^{23}$ Mx) and toroidal fields after about every ~11 y or so.
2. Phase of the reversal: ~1-2 y after sunspot maximum.
3. Poleward migrations of 'f' polarities and magnetic neutral lines (filament channels).

Sunspot Activity Cycle (Timescales $\lesssim$ 11 y):

4. Periodicity in sunspot abundance with a period ~ 11 y (Historically the first 'solar cycle phenomenon' discovered).
5. Total flux: $\sim 10^{24} - 10^{25}$ Mx.
6. Distribution:
   a) central latitudes ($\lesssim 40°$)
   b) preferred longitudes (?)
   c) butterfly diagrams
7. Properties of the 'unit' of activity (viz. a spotgroup):
   a) polarity laws
   b) orientation laws
   c) typical flux $\sim 10^{21}$ Mx

EAR and XBP Activity Cycle (Timescale $\lesssim$ 11 y):

8. Periodicity in Ephimeral Active Regions (EARs) and X-ray Bright Points (XBPs) with periods ~ 11y.
9. Phase:
   a) similar to sunspot cycle for EARs
   b) opposite for XBPs
10. Total Flux:
    $10^{25} - 10^{26}$ Mx
11. Distribution:
    a) all latitudes (pole-to-pole)
    b) no preferred longitudes (except the tendancy to avoid those occupied by spot activity)
12. Properties of the unit of activity (EAR/XBP)
    a) polarity random but often turning to normal for EARs
    b) typical flux $\sim 10^{18} - 10^{19}$ Mx

Magnetic field behaviour on smallest and medium scales length scales < R:

13. 'flux tubes' with B $\sim 10^{3}$ G; flux $\sim 10^{17} - 10^{18}$ Mx.

14. Clustering in active regions (upto $\sim 10^{22}$ Mx; typical 10^{21} Mx)
15. 'Down flows' (?) total mass supply $10^{26.5}$ gms per cycle.

Coronal Behaviour on Timescale

16. Variation of the shape and size of the corona with sunspot cycle.
17. Variation in abundance, location and sizes of coronal holes (e.g. from geomag. data)

Flows and Differential Rotation (length-scale $\lesssim R_0$):

18. Two varieties of differential rotation of magnetic structures.
19. Variation between the two with the phase of the cycle.
20. Torsional oscillations in the photospheric plasma rotation.

Timescale $\lesssim$ 22 y:

21. Relations between $(N)^{th}$ & $(N+1)^{th}$ cycle (e.g. from geomag. data)
22. Rise amplitude relations.

Timescale $\gtrsim$ 22 Y:

23. Modulation on timescales ~ 88 y.
24. Maunder minima and resurrection there from.

Long Term Behaviour:

25. Long time scale stability upto ~ 700 millioniums ago.

Appendix II

TURBULENT DYNAMO MODELS HAVE ACHIEVED AGREEMENT WITH MANY OBSERVATIONS. THEN WHY IS THE DYNAMO PROBLEM STILL UNSOLVED?

1. Agreements with observations are not from a single set of input parameters.
2. First order smoothening approximation requires $|B'| < |\bar{B}|$. But observed thin strong flux tubes imply $|B'| \approx |\bar{B}|$ if the tubes are densely packed (in which case Lorentz-forces cannot be neglected) and $|\bar{B}| > |B'|$ otherwise. Here $\bar{B}$ is the ensemble average and B' is the random part of the field.
3. Another basic assumption $\lambda >> \langle v \rangle \tau$ is not valid for the observed turbulence (Here λ is correlation length, $\langle v \rangle$ is r.m.s. velocity of turbulence, τ is correlation time).
4. No way of removing the small scale fields produced at the boundaries of the eddies.
5. Requires $d\omega/d\tau < 0$. True near top of convection zone. But buoyancy removes the field completely (if at the base of convection zone where $d\omega/d\tau > 0$ for stability, then α effect is < 0). (Here ω is angular velocity of rotation).
6. When the dynamics is introduced, the field either grows indefinitely or contradicts migrations (butterfly diagrams) and the differential rotation (Gilman and Miller, 1981).

TURBULENT DYNAMO THEORY CANNOT BE SAID TO HAVE SOLVED THE DYNAMO PROBLEM. CONTINUATION OF THINKING ON ALTERNATIVE APPROACHES IS JUSTIFIED AND MAY EVEN BE NECESSARY.

References

Babcock, H.W., 1961, Astrophys. J. **133**, 572.

Cowling, T.G., 1981, Ann. Rev. Astron. Astrophys. 19, 115.

Gilman, P.A., and Miller, J., 1981, Astrophys. J. Suppl. **246**, 555.

Gokhale, M.H., 1977, Kodaikanal Obs. Bull. **A2**, 19.
1979a, Kodaikanal Obs. Bull. **A2**, 217.
1979b, Kodaikanal Obs. Bull. **A2**, 222.

Gokhale, M.H., and Sivaraman, K.R., 1982, Bull. Astron. Soc. India. **10**, 154.

Howard, R., 1974, Solar Phys. **38**, 59.

Krause, F., and Rädler, F.H., 1980, Mean Field Magneto-Hydrodynamics and Dynamo Theory, Pergamon Press.

Layzer, D., Rosner, R., and Doyle, H., 1979, Astrophys. J. **229**, 1126.

Makarov, V.I., Stoyanova, M.N., and Sivaraman, K.R., 1982, J. Astrophys. & Astron. **3**, 379.

Makarov, V.I., and Sivaraman, K.R., 1983, Solar Phys. **85**, 215.

Parker, E.N., 1963, Astrophys. J. **138**, 226.

Piddington, J.H., 1971, Proc. Astron. Soc. Australia, **2**, 7.
1972, Solar Phys. **22**, 3.
1981, Astrophys. J. **247**, 293.
1982, Astrophys. & Space Sci. **87**, 89.

Priest, E.R., 1982, "Solar Magnetohydrodynamics", Dordrecht, D.Reidel.

Schussler, M., 1980, Nature, **288**, 150.

Stix, M., 1976, Astron. Astrophys. **47**, 243.

Yoshimura, H., 1979, Astrophys. J. **227**, 1042, and references therein.

DISCUSSION:

GOPALSWAMY: Knowing the set of observations and the parameters to be introduced, can one do an optimization?

GOKHALE: So far even the set of parameters has not been uniquely identified, and hence the question of the optimization of values does not arise. Turbulent dynamo experts must be working towards the final choice.

Kodaikanal Obs. Bull. (1984) 4, 35-42.

VECTOR MAGNETIC FIELDS IN PROMINENCES: Observations and Analysis

R.N. Smartt
National Solar Observatory
National Optical Astronomy Observatories*
Sunspot, NM 88349, U.S.A.

and

L.L. House
High Altitude Observatory
National Centre for Atmospheric Research**
Boulder, CO 80307, U.S.A.

Abstract

Measurements of the polarization of the He I D_3 multiplet in a prominence allow the magnetic fields associated with the prominence to be deduced. The amount and angle of the linear polarization are governed by the Hanle effect, the detailed theory of which is applied to the Stokes components of the He I D_3 emission to derive the associated vector magnetic fields. The dependence of the observed polarization on the magnetic field is predicted from solutions of the statistical equilibrium equations for the He I D_3 multiplet. Magnetic field vector solutions for each pair of linear polarization Stokes profiles corresponding to an observational point in a prominence are not uniquely determined. Nevertheless, physically correct solutions can usually be identified with a high confidence level. Field vectors are mostly close to horizontal and normal to the prominence surface, magnitudes ranging from 6 G to 60 G, with a mean of 24 G.

1. Introduction

The key to understanding the structure and origin of prominences lies in establishing their vector magnetic field configuration. Zeeman-effect magnetograph measurements allow only the longitudinal (line-of-sight) component of the field to be measured with reasonable accuracy (±1 G) and with a moderate sensitivity down to ~1 G, while measurements of the transverse component have an estimated sensitivity of only 50 G (Leroy, 1979), a value apparently much larger than typical field strengths within quiescent prominences. Moreover, it is now generally recognized that the validity of such measurements and the accuracy of the corresponding derived fields, interpreted by the Zeeman effect can be severely limited by resonance polarization contributions. In the case of He I D_3, for example, the observed circular polarization results both from the Zeeman effect and from level crossing interference in the Hanle effect (Landi Degl' Innocenti, 1982). Also, radiative transfer effects in commonly used lines such as H_α substantially complicate the magnetic field interpretation.

---

* Operated by the Association of Universities for Research in Astronomy, Inc. under contract AST 78-17292 with the National Science Foundation.

** The National Center for Atmospheric Research is sponsored by the National Science Foundation.

Polarization due to resonance scattering, modified by the presence of a magnetic field- the Hanle effect - is a sensitive and accurate indicator of the vector magnetic field in a prominence. The Hanle effect occurs in a weak magnetic field when the Zeeman splitting is comparable to the natural width of the component sublevels; the resulting partial degeneracy of the level mixes the polarization properties of the Zeeman sub-levels. This mixing partially depolarizes radiation and reorients the plane of polarization of radiation undergoing resonance scattering. The extent of the depolarization depends upon the magnitude and direction of the field. From the amount of the depolarization and rotation, one may deduce the vector magnetic field associated with a prominence.

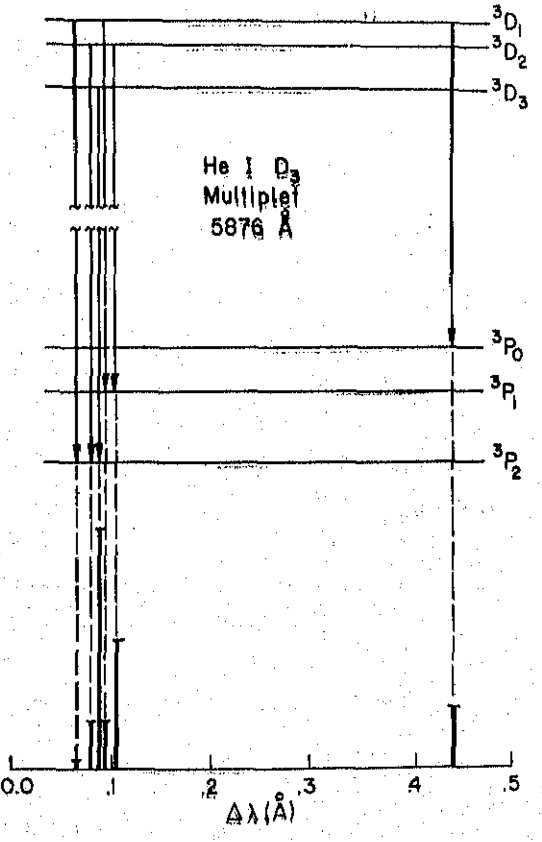

Fig.1. The relative magnitudes and spectral locations of the transitions that form the He I D_3 multiplet.

The D_3 (5876 Å) spectral profile has two well-defined components. The major (blue) component results from five transitions, 3^3D_3-2^3P_2, 3^3D_2-2^3P_2, 3^3D_2-2^3P_1, 3^3D_1-2^3P_2 and 3^3D_1-2^3P_1, while the minor (red) component is a simple triplet, 3^3D_1-2^3P_0, producing an extended wing in the profile. The peaks are separated by about 0.34 Å. The relative magnitudes and spectral locations of the D_3 transitions are shown in Figure 1. The two components of the profile have different polarization sensitivities to magnetic field strengths (House and Smartt, 1979, 1982), and if spectrally resolved and isolated by Gaussian curve fitting, two independent measurements of linear polarization (from the Q and U Stokes scans) are obtained. A histogram of linear polarization values, P(1), associated with the major component of the profile, representing 83 measurements of quiescent prominences, is shown in Figure 2a. Figure 2b is a corresponding histogram of the polarization, P(2), of the minor component revealing the significantly different distribution of P(1) and P(2). This difference in sensitivity produces some redundancy (for

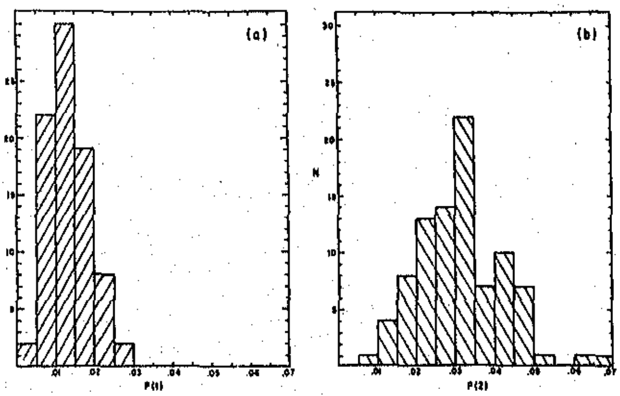

Fig.2. Histograms of the linear polarization, P, as observed in quiescent prominences corresponding to a) the major component of the D_3 profile (P(1)), and b) the minor component of the D_3 profile (P(2)).

perfect data) in the information required to deduce the vector field. Further, Landi Degl' Innocenti (1982) has completed the theory of D_3 by computing the expected circular polarization profile for a given configuration of the magnetic field vector. The observed circular polarization V profiles can then be interpreted. Since the resultant data from the V profiles are independent, ambiguities intrinsic to interpreting polarimetric data of prominences in D_3 can be resolved. However, observationally the V_0 component is frequently noise-dominated and hence uninterpretable. Additional advantages of D_3 are that it is both optically thin and relatively bright in prominences. Most importantly however, the statistical equilibrium equations have been solved in sufficient detail (Bommier et al. 1981: Landi Degl' Innocenti, 1982) that D_3 may be interpreted with confidence. Here we report on measurements of vector magnetic fields associated with a quiescent prominence, obtained by interpeting spectrally resolved Stokes scans of D_3. For a more detailed description of this work, refer to House and Smartt (1982), Athay et al. (1983) and Querfeld et al. (1984).

2. Observations

The D_3 polarimetric observations of the prominence discussed here were obtained on April 19-22, 1978, using the HAO/SPO Stokes-I polarimeter (Baur et al. 1980). A set of Stokes profiles, coresponding to one observational point (3.5 arc sec x 10 arc sec), represents 100 spectral scans recorded in about 20 minutes. The dispersion of the prominence in both H_α and D_3 on four consecutive days of observations, as well as on April 23, is shown in the spectroheliograph images of Figure 3 (at approximately 14:00 UT). Note the significant evolution of the prominence over a four-day period. This prominence occurred in the S-E, extending in longitude over

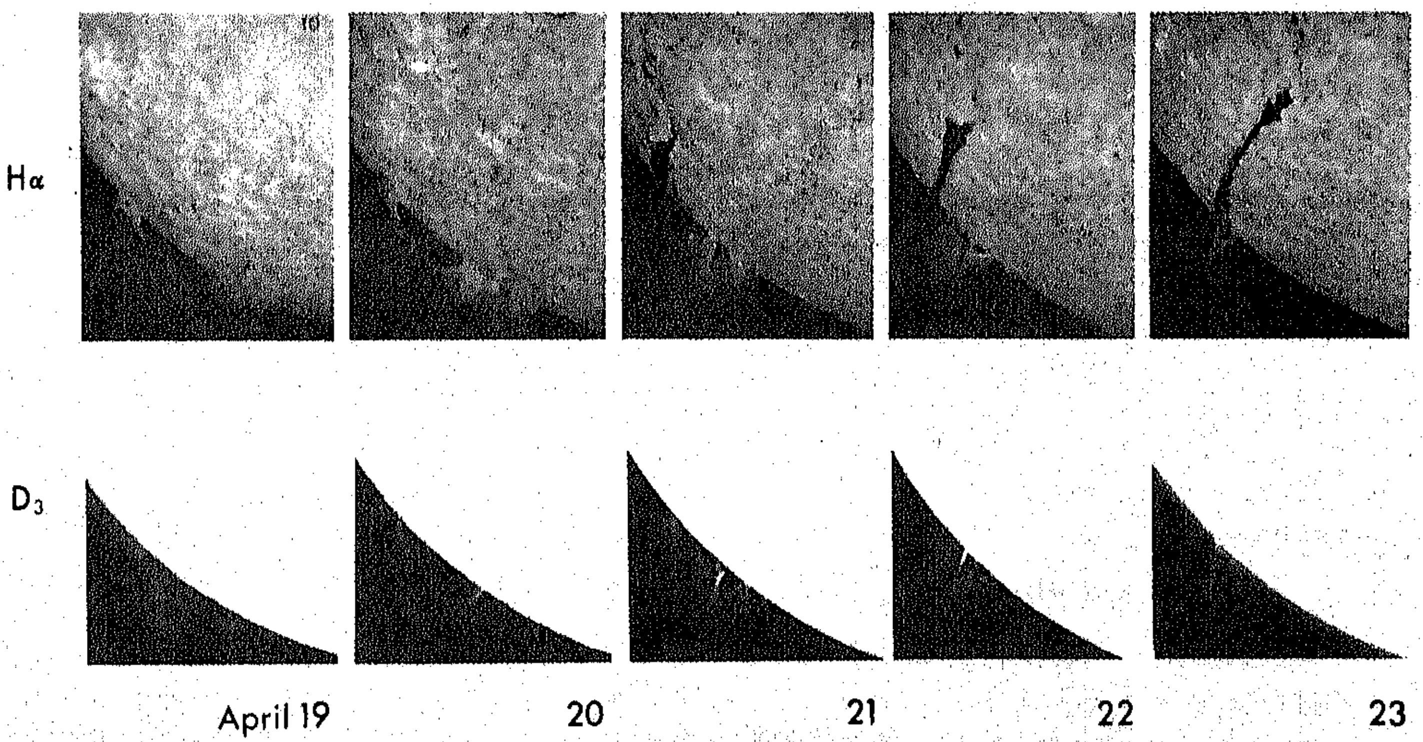

Fig.3. Spectroheliograph images in H_α and D_3 of a large quiescent prominence of which polarimetric observations were obtained, April 19-22, 1978. Approximately one hour after the last image was recorded, the prominence erupted.

about 75°, and in latitude from approximately 31° to 52°. The long axis of the prominence was inclined by about 30° to the line of sight. The maximum height was ~ 10^5 km. This prominence erupted abruptly soon after 14:00 UT on April 23.

A sample of a typical set of four D_3 Stokes spectral profiles, intensity, I, linear polarization, Q and U, and circular polarization, V, is shown in Figure 4. The ordinate units are millionths of the central disk spectral brightness. The linear polarization degree (of the major component) is about 2% while the circular polarization is a factor of four smaller. Instrumental noise levels were below 10^{-3} in polarization. Note that a two-slit magnetograph measurement of V would be very misleading.

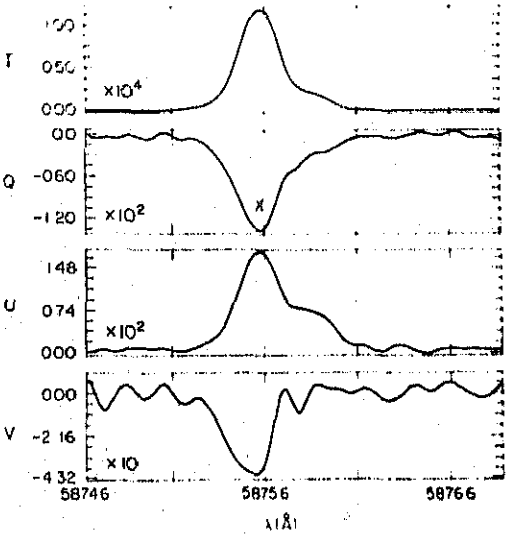

Fig.4. A typical set of Stokes profiles in D_3.

3. Data Processing

Polarimetric observations such as those shown in Figure 4 are initially smoothed and fitted with Gaussians to obtain the relevant polarization parameters. As well, they must be augmented with supplementary information necessary for their interpretation.

The polarization reference axis assumed in both the Bommier (1981) and Landi Degl' Innocenti (1982) statistical equilibrium solutions lies along the local radius so that Q and U must be rotated from the instrument coordinates, E-W geocentric, into the radial reference frame. In addition, the apparent height, h, of the observation above the limb and the dihedral angle, χ, between the plane of the sky and the heliocentric radius through the observed point are necessary. h and χ together give the true height, $r = (R_0 + h) \cos \chi$. The angle χ is also needed to determine the disk-prominence-observer scattering angle. The measurement of χ is invariably uncertain. It is best obtained by tracking a specific point on the prominence over a period of time. Such a sequence of observations, ideally over several days, even if available, has limited precision due to the general evolution in form of all prominences even on a time scale of a few hours.

All of the amplitudes for I, Q, U and V are normalized to the intensity to obtain blue and red values of Q/I, U/I, and V/I, proportional to the integrated strengths of the multiplet components. This results in four linear polarization values $(Q/I)_{red}$, $(Q/I)_{blue}$, $(U/I)_{red}$, $(U/I)_{blue}$, which are used to obtain plausible, but usually ambiguous values for field strengths, $|\underset{\sim}{B}|$, and direction (θ, ϕ), where θ is the field polar angle measured from the local radius and ϕ is the azimuthal angle measured around the local radius, with $\phi = 0°$ pointing west and $\phi = 90°$ pointing north. The remaining data, $(V/I)_{blue}$ and $(V'/I)_{blue}$ (where V' is the derivative of V) are used to reduce the ambiguities inherent in the Q, U interpretation.

3.1. Hanle Effect Codes for He I D_3

Bommier et al. (1981) and Landi Degl' Innocenti (1982) have independently constructed Hanle effect codes for the magnetic field interpretation of prominence Stokes profiles in He I D_3.

From the Stokes profiles, the observational parameters of intensity and the corresponding two-dimensional linear polarization vectors for both the blue and red components of the D_3 multiplet, as well as values for h and χ , are employed in the interpretation.

Essentially two sets of equations must be solved. The first relates the density-matrix components of the atomic system to the properties of the incident radiation field and the second describes the properties of the emitted radiation in terms of the density matrix. An inversion procedure, incorporating a transformation from the coordinate system used conventionally in the theory to that of the instrument, is then used to determine corresponding magnetic field values. The Bommier code simplifies the computational procedure by calculating the field for a height of 50 arc sec and scaling this value for any given observational height, whereas the Landi Degl' Innocenti code computes $\mathbf{B}$ in increments of 10 arc sec in height, and interpolates between heights. The Landi Degl' Innocenti code also incorporates an interpretation of Stokes V-profile data, which consists of an independent intensity-like component, $\phi(\lambda)$, and a Zeeman component, $\delta\Phi/\delta\lambda$ (Landi Degl' Innocenti, 1982). This interpretation proves to be cruical in sifting out a single value for the magnetic field from a typical set of solutions, as discussed in Section 4 below. Since the Bommier code was available in a fully-developed form, it was used almost exclusively for the results reported here.

4. Results

4.1. Multiple Solution and Sifting Procedures

It has been verified that synthetic linear polarization data, used as input, result in unique magnetic field vector solution, or at most a symmetrical pair of solutions. The ambiguity is intrinsic to scattering polarization in the presence of a magnetic field (see Landi Degl' Innocenti, 1982). However, when observational data are used multiple-valued solutions are generally produced that satisfy the fundamental requirement that a vector magnetic field predicted by one component of the D_3 profile is also predicted by the other. The inversion procedure of the code searches for the best solutions based on this criterion, in terms of a so-called distance function, D, where

$$D = \sqrt{\sum_i [(\Delta Q_i)^2 + (\Delta U_i)^2]}$$

and where $Q_i = (Q_i\text{theo} - Q_i\text{obs})/I$, the summation index running on the two components of D_3 line. The lack of uniqueness apparently result from residual noise, spatial and temporal averaging and imprecision in the geometrical parameters, all inherent in the observational data.

Various procedures have been used to sift out invalid solutions. The most straight forward is where the V-profile is well defined. Theoretical V-profiles can be constructed from the linear polarization solutions and compared with the observed profiles. This procedure can be sufficient to isolate the correct solution. As pointed out in the previous section, the V-profile consists of a component proportional to intensity and a Zeeman component, proportional to the derivative of the intensity, the two components denoted here by V and V', respectively. The presence of V' therefore is evidence of a longitudinal component of the field and its absence that the field is very nearly transverse. Further, the signs of Q, U, V and V' can be compared for self-consistency for a given set of B, h and χ, and many solutions rejected on this basis. As an extension of this procedure, polarization maps for Q, U, V and V', for both components, so-called altitude diagrams, have been prepared. These are contour maps of polarization on a θ, ϕ plane for a given B, h, χ set. By intercomparing a set of corresponding maps, inadmissible solutions can be readily identified.

By such methods, it is frequently found that all tentative solutions can be eliminated except a symmetrical pair. The correct direction can then be identified, at least with modest confidence, by comparison with photospheric magnetic fields. Uncertainty arises primarily from the possible substantial evolution of a field distribution between the time of the prominence observations and that of the magnetograph record. Finally, self-consistency provides a further, general check on the validity of a set of solutions representing measurements in the same prominence, especially if such measurements are repeated on two or more days.

4.2. Summary of Magnetic Field Solutions

The prominence measurements discussed here constitute a particularly useful set in that the profiles are generally of good quality (36 of 44 of the observed points are interpretable in the linear polarization) and extend over four consecutive days, during which time the prominence gradually evolved in form and systematically increased in height. Since this prominence was relatively high and extensive and was observed over a four-day period, estimates of h and χ could be obtained with more confidence than for typical prominences.

The complete set of magnetic field vector solutions are presented in Figure 5. The dashed outline of the prominence, imprecise because of the changing form of the prominence over the four-day period, is intended to give simply a general frame of reference. Note the tendency for large values of $|\underset{\sim}{B}|$ to occur in the leg of the prominence and that most of the remaining above-average values occur in the central part of the bulk of the prominence. The mean value is 23.8 G.

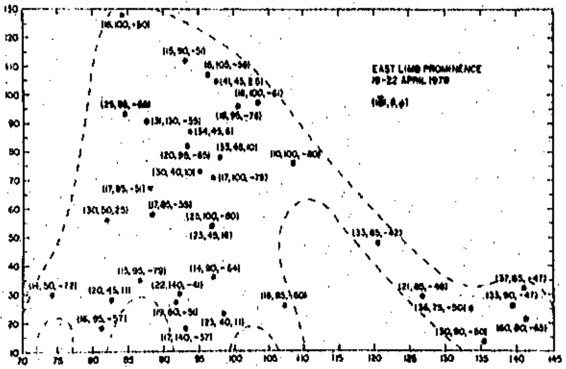

Fig.5. Vector field orientations and positions in the 19-22 April, 1978 quiescent prominence. The number sets are field strength, B (gauss), the polar angle, θ (degrees), measured from the local radius, and the azimuthal angle, ϕ(degrees), around the local radius. Zero azimuth points west, +90° points north.

Figure 6 is a latitude-longitude plot of field vectors for the same data set of

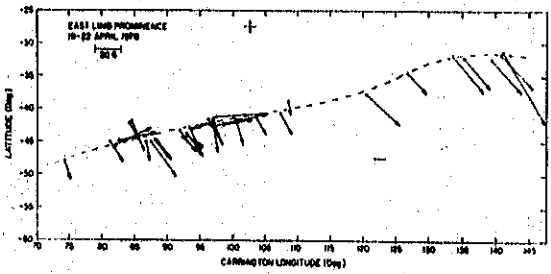

Fig.6. Latitude-longitude plot of field vectors for the 19-22 April, 1978 prominence. Arrows are proportional to the field strength. Surface magnetograph polarities are shown.

Figure 5. The length of the arrows are proportional to the field strength. The dashed line represents an approximate outline of the prominence as seen as a filament. The plus and minus signs indicate the surface magnetograph polarities. With some marked exceptions, the tendency for the horizontal component of the field vector to lie close to 90° from the long axis of the prominence is obvious.

5. Comments

It has been pointed out above that the polarimeter field aperture, 3.5 arc sec by 10 arc sec, is large compared to the fine threads of emitting material, ~1 arc sec or smaller, that are sometimes observed in high resolution images of prominences. If such threads represent corresponding fine-scale magnetic structure, rather than simply being evidence of thermal instabilities, the observed mean polarization would be larger than that representative of the magnetic elements and the magnitude of the deduced magnetic field values would be correspondingly reduced. Implicit in the procedure for magnetic field derivation then is the assumption that the magnetic field is homogeneous over the polarimeter angular aperture. But even if the magnetic field is uniform over the field sampled by the polarimeter, line of sight contributions are likely to have a mixture of field components, which would result in a diminution of observed polarization and an increase to an unknown degree of inferred field strengths. The further assumption that the prominence material is effectively stationary during the period of observation is also not necessarily valid, and if so, the effect is also to increase the inferred field strengths.

Conclusion

Stokes polarimeter spectral profiles of He I D_3, representing many observational points within a quiescent prominence, have been interpreted using a detailed quantum-mechanical theory of resonance polarization for the D_3 multiplet. The multiple set of solutions obtained when the linear polarization information alone is used can be reduced, generally to a symmetric pair, when the full, generalized theory is applied that interprets also the weak circular polarization Stokes profile. In most cases a unique solution can be found through additional information available from disk field polarity.

Most of the derived magnetic field vectors are close to horizontal and near normal to the prominence surface, with some extreme exceptions, thus generally supporting the Kippenhahn-Schluter (1957) model. The values obtained for the magnetic field vectors are thought to be mostly accurate representations of the actual prominence fields, a mean for this prominence of 24 G.

References

Athay, R.C., Querfeld, C.W., Smartt, R.N., Degl' Innocenti, E.L., and Bommier, V., 1983, Solar Phys. 89, 3.

Baur, T.G., House, L.L., and Hull, H.K., 1980, Solar Phys. 65, 111.

Bommier, V., Leroy, J.L., and Sahal-Brechot, S., 1981, Astron. Astrophys. 100, 231.

House, L.L., and Smartt, R.N., 1979, in E. Jensen et al. (eds), "Physics of Solar Prominences", Institute of Theoretical Astrophysics, Oslo, p.81.

House, L.L., and Smartt, R.N., 1982, Solar Phys. 80, 53.

Kippenhahn, R., and Schluter, A., 1957, Z. Astrophys. 43, 36.

Landi Degl' Innocenti, E., 1982, Solar Phys. 79, 291.

Leroy, J.L., 1979, in E.Jensen et al. (eds), "Physics of Solar Prominences", Institute of Theoretical Astrophysics, Oslo, p.56.

Querfeld, C.W., Smartt, R.N., Bommier, V., Landi Degl' Innocenti, E., and House, L.L., 1984, (Submitted to Solar Phys.)

DISCUSSION:

BHATTACHARYYA: (1) How do you calculate the strength of the magnetic field? Are there any calibrations from laboratory measurements?

SMARTT: (1) The strength of the magnetic field is calculated by applying the theory of the Hanle effect for He I D_3 line to the observed polarization. There has been no laboratory verification.

BHATTACHARYYA: (2) Cannot one measure the field in prominences by Zeeman method?

SMARTT: (2) Earlier attempts to measure magnetic field strengths in prominences based on the Zeeman effect, one now recognized as being invalid due to the dominence of the Hanle effect in the magnetic field regime appropriate for prominences, and especially so for lines which are not optically thin in prominences.

VINOD KRISHAN: Have there been any attempts to produce analytic functional forms of the magnetic field from the derived numbers?

SMARTT: So far, we have obtained only the vector magnetic field functions. We plan to investigate statistical relationships of the cumulative data and especially to use this information to try to understand the observed morphology of quiescent prominences.

Kodaikanal Obs. Bull. (1984) 4, 43-46.

MODELLING OF PLASMA STRUCTURES IN THE SOLAR ATMOSPHERE

V. Krishan
Indian Institute of Astrophysics
Bangalore 560034
INDIA

Abstract

A maximal helicity principle is proposed to study the stability of plasma structures in the solar atmosphere. This principle derives from the statistical treatment of the magnetohydrodynamical turbulence. The steady state of the plasma system results from subjecting the system to the invariance of total energy, the magnetic helicity and toroidal and poloidal magnetic fluxes. The statistical distributions of the velocity and magnetic fields are formulated.

1. Introduction

High resolution optical, UV, EUV and X-ray observations have established the spatial complexity of the solar corona. Active regions appear in the form of loops or arches. The spatial structure of these loops outlines the magnetic field geometry. From the observations of lines of Ca II, HI, CII, CIII, CIV, Ne VII, Mg VIII, Mg IX and Mg X, it is concluded that the loops consist of a cool core surrounded by a hot sheath which merges with the hot corona, Vaiana and Rosner (1978).

2. Maximal Helicity Principle for Stability

We assume plasma to be in the form of a cylinder of radius R and length L with rigid perfectly conducting walls at $r = R$. The MHD equations for an incompressible medium are:

$$\rho\left[\frac{\delta\vec{v}}{\delta t} + (\vec{v}.\vec{\nabla})\,\vec{V}\,\right] = \frac{1}{4\pi}\,(\vec{\nabla}\times\vec{B})\times\vec{B}-\vec{\nabla}p+\rho\vec{g} \qquad (1)$$

$$\frac{\delta\vec{B}}{\delta t} = \vec{\nabla}\times(\vec{V}\times\vec{B}), \quad \vec{\nabla}.\vec{V} = \vec{\nabla}.\vec{B} = 0 \qquad (2)$$

where, the symbols have their usual meaning. The boundary conditions on B and V are:

$$V_r\ (r=R) = 0 = B_r\ (r=R) \qquad (3)$$

The geometry is indicated in Fig.1.

Using the incompressibility condition in the divergence of equation (1), one gets a relation between p, V and B as:

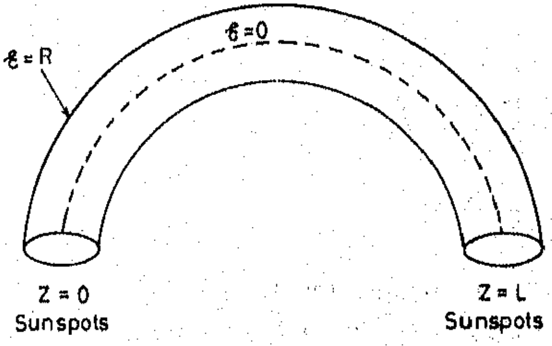

Fig.1. The geometry of a solar corona loop.

$$\nabla^2 p = 1/4\pi\ \nabla.[(\nabla \times B) X B] - \nabla.[\rho(\vec{V}.\vec{\nabla})V] + \nabla.(\rho\vec{g}) \tag{4}$$

which determines the density and temperature profile of the plasma. The three invariants of the plasma system are:

Total energy $E = \int d^3 X\ (V^2 + B^2)$ (5)

Magnetic helicity $H_M = \int d^3 X\ \vec{A}.\vec{B}$ (6)

Cross helicity $H_C = \int d^3 X\ \vec{V}.\vec{B}$ (7)

The poloidal flux $\psi_p = \int_0^L dz \int_0^{2\pi} d\theta\ A_z$

$= \text{constant at } r = R$ (8)

where $\vec{A}$ is the vector potential.

The velocity and magnetic fields are expanded in terms of Chadrasekhar-Kendall functions given as:

$$\begin{aligned}\vec{a}(n,m,q) &= e_r\left[\frac{im}{r} + \frac{ik_n}{\lambda(n,m,q)}\frac{\delta}{\delta r}\right]\psi(n,m,q)\\ &+ e_\theta\left[\frac{\delta}{\delta r} - \frac{mk_n}{r\lambda(n,m,q)}\right]\psi(n,m,q)\\ &+ e_z\left[\frac{\lambda^2(n,m,q) - k_n^2}{\lambda(n,m,q)}\right]\psi(n,m,q)\end{aligned} \tag{9}$$

where

$\psi(n,m,q) = J_m(\gamma_{nmq}\ r)\ e^{im\theta + ik_n z}$

$\lambda(n,m,q) = \pm[\gamma_{nmq}^2 + k_n^2]^{1/2}$

$K_n = \frac{2\pi n}{L}$; $n=0, \pm 1, \ 2, \ldots\ldots\ldots\ldots;$

$m=0, \pm 1, \pm 2, \ldots\ldots\ldots\ldots,$

γ_{nmq} corresponds to that solution which makes $\vec{a}$ satisfy the boundary condition $a_r = 0$ at $r = R$. This gives for $m^2 + \eta^2 > 0$.

$$Rk_n\ \gamma_{nmq}\ J'_m(\gamma_{nmq} R) + m\lambda(n,m,q)\ Jm(\gamma_{nmq} R) = 0 \tag{10}$$

The eigen values for $m = n = 0$ are determined from the ratio of toroidal to poloidal flux:

$$\frac{\psi_t}{\psi_p} = \frac{-R}{L}\ \frac{\gamma_{ooq}\ J'_O\ (\gamma_{ooq} R)}{\lambda(o,o,q)\ Jo(\gamma_{ooq} R)} \tag{11}$$

Now, all the fields and the invariants can be expressed in terms of $\vec{a}$ by using

$$\vec{B} = \sum_{n,m,q} Cnmq\ \lambda(n,m,q)\ \xi(n,m,q)\ \vec{a}(n,m,q) \tag{12}$$

$$\vec{V} = \sum_{n,m,q} Cnmq\ \lambda(n,m,q)\ \eta(n,m,q)\ \vec{a}(n,m,q) \tag{13}$$

The statistical mechanics of the V and B fields is then formulated in a phase space whose coordinates are the real and imaginary parts of ξ'S and η'S. The most probable state of the system is then constructed subject to the constraints of conservation laws. This leads to a canonical ensemble which has an exponential term having a lagrange multiplier for every conserved quantity. Lagrange multipliers are determined by requiring a given value of the expectation value of the conserved quantity, Montgomery et al. (1978). One chooses the canonical distribution subject to the invariance of E, H_M, H_C, ψ_t and ψ_p as:

$$D = \text{Constant} \exp\ [-\alpha E - \beta H_M - \gamma' H_c - \delta\psi_t] \tag{14}$$

where α, β, γ' and δ are the Lagrange multipliers. For initially quiescent conditions $H_C = 0$ and, therefore $\gamma' = 0$. One can factor out the probability distribution for each expansion coefficient. The probability distribution for η(n,m,q) is:

$$P\eta(n,m,q) = Kn,m,q \exp\ [-\alpha\lambda^2(n,m,q)\ |\eta(n,m,q)|^2\ ] \tag{15}$$

From this we find

$$< |\eta(n.m.q)|^2 > = \alpha^{-1}\ \lambda^{-2}(n,m,q) \tag{16}$$

Similarly, one can carry out the procedure for other coordinates ξ(n,m,q). One notices from equation (16) that even for initially quiescent conditions there is a finite mean square velocity for every mode in the system. Four scalar quantities, $<E>$, $<H_M>$, $<\psi_t>$ and $<\psi_p>$ are sufficient to determine the level of excitation of every mode in the system.

3. Application to Coronal Loops

3.1. Radial Temperature Variation

We propose that the steady state of the loop can be described in terms of a single Chandrasekhar-Kendall function characterized by m = n = 0. Equation (4) for this choice can be solved to find the radial variation of the plasma temperature as:

$$T(r) = \frac{m_i}{k_B} \lambda^4 (0,0,1)|\eta^2(0,0,1)| \; C^2(0,0,1) \; X$$

$$[\, x \{ J_0^2(x) + J_1^2(x) \} - J_1(x) \, Jo(x)] + To \quad \text{and}$$

$$\frac{\delta T}{\delta r} = \frac{m_i}{k_B} \lambda^5 (0,0,1) \, |\eta^2 (0,0,1)| \; C^2(0,0,1) \; X$$

$$\frac{J_1^2(x)}{x} \tag{17}$$

where $T = T_0$ at $r = 0$; $x = \lambda r$, λ is determined from equation (11). One can substitute for T(r) from eq. (17) in the line flux calculations and determine the spatial widths of the lines CII, CIII, OIV, OVI, Ne VIII and Mg X which have mean temperatures of formation $5x10^4$K, $9x10^4$K, $2x10^5$K, $3x10^5$K, $6x10^5$K and $1.4x10^6$K respectively. Now $\lambda^2\eta^2$ (0,0,1) is a measure of the turbulent velocity in the fluid and can be estimated from the observed Doppler widths of these lines. For $\lambda^2\eta^2 \sim 10^{14}(\text{cm/sec})^2$ and $T_0 = 6x10^3$K, $\lambda = 2/R$, $R = 10^9$cm, $B \sim 1.5$ Gauss, we find the spatial widths to be $0.02\,\lambda^{-1}$, $0.025\,\lambda^{-1}$, $0.12\,\lambda^{-1}$, $0{,}1215\,\lambda^{-1}$, $0.3\lambda^{-1}$ and $> 0.5\lambda^{-1}$ for CII, CIII, OIV, OVI, Ne VII and Mg X respectively. This behaviour certainly conforms to the cool core and hot sheath type of loops.

3.2. Statistical Mechanics of V and B Fields

In order to formulate the statistical mechanics, we include two values of the parameter q which labels the various roots of equation (11) as λ_0, λ_1, etc. One can express the average values of E, H_M and ψ_t in terms of λ'S and the Lagrange multipliers. The Lagrange multipliers can be solved for by assigning some given values to $<E>$ $<H_M>$, $<\psi_t>$ and $<\psi_p>$. As a numerical example, say $L = 5x10^9$cm, $\psi_t/\psi_p = 1$ then equation (11) gives $\lambda_0 = 2.2/R$ and $\lambda_1 = -2.6/R$. The values of α , β and δ are determined from the following relationships:

$$\alpha = [2(\bar{E}-\lambda_1\bar{H}_m) \; (\bar{E}-\lambda_1\bar{H}_m)]^{-1} \; X$$

$$[\, - \{ -3\bar{E} + \frac{3}{2}(\lambda_0 + \lambda_1) \; \bar{H}_m \} \; \pm$$

$$\{ \bar{E}^2 - \frac{9}{4}(\lambda_0 + \lambda_1)^2 \; \bar{H}_m^{-2} - 8\lambda_1\lambda_0 \, \bar{H}_m^{-2}$$

$$- \bar{E}\,(\lambda_0 + \lambda_1) \; \bar{H}_m \}^{1/2} \,] \tag{18}$$

$$\beta = \frac{\lambda_1}{2(\bar{E} - 1/\alpha - \lambda_1\bar{H}_m)} - \frac{\lambda_0}{2(\bar{E} - 1/\alpha - \lambda_0\bar{H}_m)} \tag{19}$$

and

$$\delta = \bar{\psi}_t \, [\frac{\delta_0^2 \, (\bar{E} - 1/\alpha - \lambda_1 H_m)}{\lambda_0(\lambda_0 - \lambda_1)}$$

$$+ \frac{\delta_1^2 \, (\bar{E} - 1/\alpha - \lambda_0\bar{H}_m)}{\lambda_1(\lambda_1 - \lambda_0)}]^{-1} \tag{20}$$

where $\delta_0 = 2\pi RC(0,0,1) \; \gamma_{001} \, J_1(\gamma_{001}R)$

$\delta_1 = 2\,RC(0,0,2) \; \gamma_{002} \, J_1 \, \gamma_{002}R)$

$\bar{E}$, $\bar{H}_M$ and $\bar{\psi}_t$ are the observables. Since for the case of coronal loops, there are no direct measurements of these quantities, we shall have to fix their values from other considerations. For example $\bar{E}$ can be obtained from energy balance arguments which give $\bar{E} \sim 10^{28}$ ergs (Levine and Withbroe 1977). We choose $H_M \sim 0.05 \times 10^{37}$ ergs cm. The two values of α are $\sim 2.04 \times 10^{-28}$ (ergs)$^{-1}$ and 0.98×10^{-28} (ergs)$^{-1}$. We find $\alpha \sim 2.04 \times 10^{28}$ (ergs)$^{-1}$ to be appropriate for the approximations involved in arriving at (18). Eq. (19) gives $\beta \approx 0.2 \times 10^{-37}$ (ergs cm)$^{-1}$, and $\delta = 10^{-36}\,\bar{\psi}_t$ (Gauss cm^2)$^{-1}$. A representative choice of $\bar{\psi}_t \sim 10^{17}$ Maxwell gives $\delta \approx 10^{-19}$. Thus the distribution function for this particular indicative example is :

$$D = \text{Const}\ e^{-2.04\bar{E}/E}\ e^{0.01\bar{H}m/Hm} \times e^{-0.01\psi_t/\bar{\psi}_t} \qquad (21)$$

We observe that total energy has a rather narrow distribution compared to the distributions of the magnetic helicity and toroidal flux. More details about the application to coronal loops are presented in the paper by Krishan (1983a,b).

References

Krishan, V., 1983a, Solar Phys. 88, 155.

Krishan, V., 1983b, Statistical Mechanics of Velocity and Magnetic Fields in Solar Active Regions (Accepted in Solar Phys.)

Levine, R.H. and Withbroe, G.L., 1977, Solar Phys. 51, 83.

Montgomery, D., Turner, L. and Vahala, G., 1978, Phys. Fluids, 21, 757.

Vaiana, G.S. and Rosner, R., 1978, Ann. Rev. Astron. Astrophys. 16, 393.

Kodaikanal Obs. Bull. (1984) 4, 47-54.

OBSERVATIONS ON THE FINE STRUCTURES IN SOLAR DECAMETRIC RADIO EMISSION

N. Gopalswamy, G. Thejappa and Ch.V. Sastry
Indian Institute of Astrophysics
Bangalore 560034
INDIA

and

Raman Research Institute
Bangalore 560080
INDIA

Abstract

The solar decametric radio emission consists of a variety of fine structures. This reflects the complexity of the corona at this level. Two observations, viz. absorption bursts and short duration narrow band bursts are presented. An interpretation of each of these observations is provided.

1. Introduction

The solar decametric radiation emanates from the region of 1-2 solar radii. The decametric noise storms consist of a continuum which may last for one to several hours. Superimposed over this continuum are a variety of fine structures. The most often observed features are the type III, type IIIb, drift pairs, S bursts and so on (Sawant 1982). However, there are large periods of time when the continuum alone is observed (Gergely and Kundu 1975). In addition to the above mentioned fine structures, Sastry et al. (1983) observed sudden reductions in the decametric continuum called the absorption bursts. Also, short duration narrow band bursts which have a small drift rate were observed recently (Gopalswamy et al. 1983b). In this paper, we discuss the absorption bursts and the short duration narrow band bursts and provide a physical interpretation for them. These observations provide information about the complex magnetic structure in the outer corona. The decametric corona is one region to which sufficient attention has not been paid. The significance of this region is reflected in the following facts: (i) the co-rotation of the corona ceases at this level (ii) the magnetic field configuration changes predominantly from closed to open field structures (iii) new spectral features appear which are absent in the higher frequency region.

Our observations do not always have flare associations. Hence, the physics of these observations pertains to the 'quiescent' corona by which we mean that the changes in magnetic field are small and may correspond to the signatures of an evolving active region. The examples we are considering seem to reflect the 'transition' character of the magnetic field in the decametric corona. The short duration narrow band bursts which occur relatively rarely may correspond to the existence of closed magnetic field configurations while the absorption bursts indicate open field lines. Both these configurations are possible as it is a transition region.

2. Absorption Bursts

2.1. Observations

The absorption bursts are seen as dips in the continuum flux for a short duration. Detailed observations are provided elsewhere (Sastry et al. 1983, Gopalswamy et al. 1983a). The most important characteristics can be summarised as follows:

(i) The absorption duration, on an average is about 2-3s,

(ii) The absorption bursts occur over a relative bandwidth of about 5%,

(iii) The absorption bursts do not have any drift in the frequency time plane,

(iv) Large number of absorption bursts have a simple time structure. However, there are double and triple structures observed and sometimes multiple time structures,

(v) The intensity reductions are $\gtrsim$ 40%.

Typical examples are shown in Fig.1. The frequency observed is around 34.5 MHz.

2.2. Interpretation

The sudden reductions are also observed in high frequency levels. (e.g. Benz and Kuijpers 1976, Fokker 1982). The cause of absorption depends upon both the generation and propagation characteristics of the continuum radiation. Since the radiation generation and their propagation outwards are different at different frequency regions, the interpretation should take account of these facts. So, one can classify the interpretations into two catagories:

(i) Absorption at the generation stage where the process of plasma wave generation or the process of conversion of plasma wave into electromagnetic radiation could be stopped temporarily to cause the observed reduction,

(ii) Absorption could be attributed to the propagation effect in that a

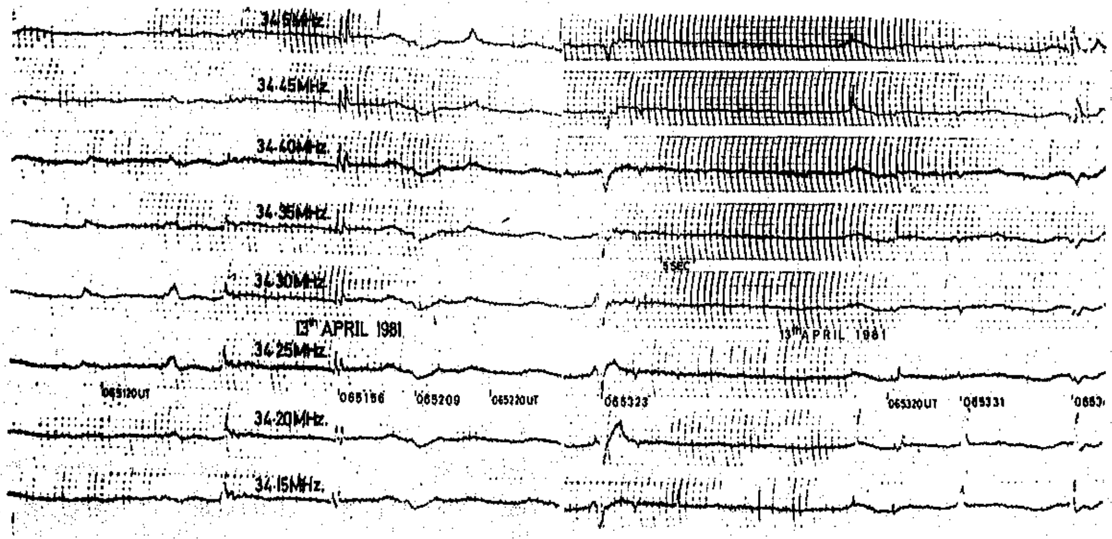

Fig.1. Eight channel record of absorption burst obtained on April 13, 1981. The ordinate is the intensity of radio emission. The absorption bursts are at 065323 UT and 065209 UT.

'screen' is present on the path of the radiation for a short while that causes the intensity reduction.

Benz and Kuijpers (1976) regarded that the sudden reduction in the decimetric continuum must be due to filling of loss cone of electron distribution trapped in the closed magnetic configuration which caused the decimetric continuum. While the loss cone is filled by the newly injected electrons, the loss cone instability for plasma waves is stopped and hence one sees a reduction in the radiation. Fokker (1982) pointed out the drawback of Benz and Kuijper's theory and proposed that the reduction could be due to inhomogeneities created on the path of radiation by solitons or shocks which impinge on the flux tubes into which the continuum radiation is ducted. The problem with Fokker's idea is that it needs open flux lines at decimetric levels which are quite rare.

If one wants to apply these theories to decametric continuum, one faces many difficulties. The decametric continuum is explained as a result of the Rayleigh scattering of enhanced plasma fluctuations caused by a diffuse electron beam along open magnetic field lines (Levin 1982). Since the theory of Benz and Kuijpers needs a closed field configuration, the loss-cone filling mechanism is not appropriate here. Fokker's (1982) idea contains the correct ingredients but one has to be sure of the ducting of continuum radiation at decametric region. There is no concrete evidence for the existence of low density plasma in the coronal streamers to cause the radiation ducting. Moreover, the inhomogeneities created by shocks are solitons of small scale lengths which may not be able to reduce the flux by 50%. Adhering to the idea of Fokker (1982) one must consider an important aspect of the shock waves such as the creation of low frequency turbulence in the shock front and its wake (Galeev, 1976). The extent over which the plasma turbulence exists is sufficiently large ($\sim 10^9$ cm) so that the large decametric continuum source of size 10' (Kundu, 1983) could be screened temporarily. When the continuum radiation passes through this region of turbulence, it interacts with low frequency turbulence (ion-sound turbulence is the one generated in the shock front and exists in the wake with a high level of energy density). The result is the generation of Langmuir waves at the expense of the continuum radiation. Once the Langmuir waves build up to a certain level, the reverse interaction of generation of radiation becomes important and hence the saturation occurs in the absorption. The ion-sound turbulence decays because there is no free energy available for its generation after the shock passage. Once the intensity of ion-sound turbulence falls below a critical level, there is no effective conversion of continuum radiation into Langmuir waves and hence the intensity recovers to the original continuum level. This critical level of ion-sound turbulence could be estimated from the requirement that the optical depth of the turbulence layer exceeds unity. From weak turbulence theory one can obtain the optical depth of the turbulence layer and calculate the critical level in terms of the effective temperature T_s of the ion-sound turbulence: $T_s > 2.4\times10^9$K. From the observed bandwidth and the scalelength of coronal inhomogeneity, one can obtain the linear extent of the turbulence layer as $\sim 10^9$ cm. The collisional damping time of the ion-sound turbulence is in the right range of observed duration of absorptions.

The non-drifting character of the absorptions support the fact that shock waves are propagating perpendicular to the radial magnetic field and hence perpendicular to the line of sight. A schematic model is proposed in Fig.(2), for the origin of such a shock wave. When an emerging magnetic field line opens in a neighbouring site, it can drive a low Mach number shock across the open field lines. The multiple fine structures could be interpreted as the passage of successive shocks. The different time structures would then correspond to the different time intervals between successive shocks. The mathematical details have been given by Gopalswamy et al.(1983a).

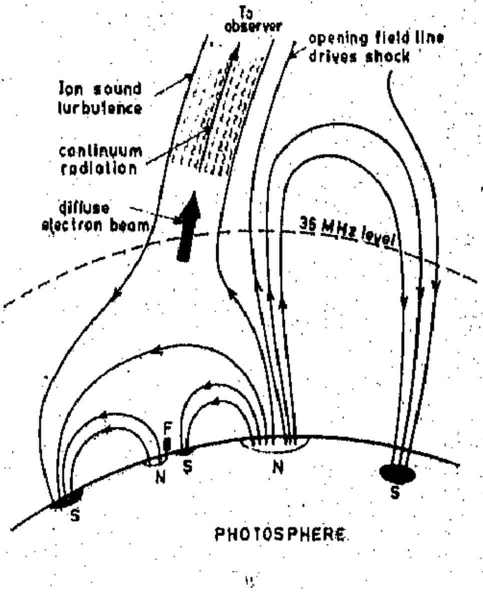

Fig. 2. A model for the absorption process.

If the shock propagates through the source region itself, then the enhanced plasma fluctuations will get converted into radiation which propagates perpendicular to the line of sight and hence one can observe a reduction in the continuum flux.

3. Short-duration Narrow-band Bursts

3.1. Observations

The short-duration narrow band bursts are identified as type I bursts at low frequencies. The solar origin of these bursts is established in several ways. Interference due to lightning, static ignition, etc. are of broad band with zero frequency drift. The broadcast interference is of narrow band but again, it has no frequency drift. The characteristics of these bursts could be summarised as follows: (see Fig.3).

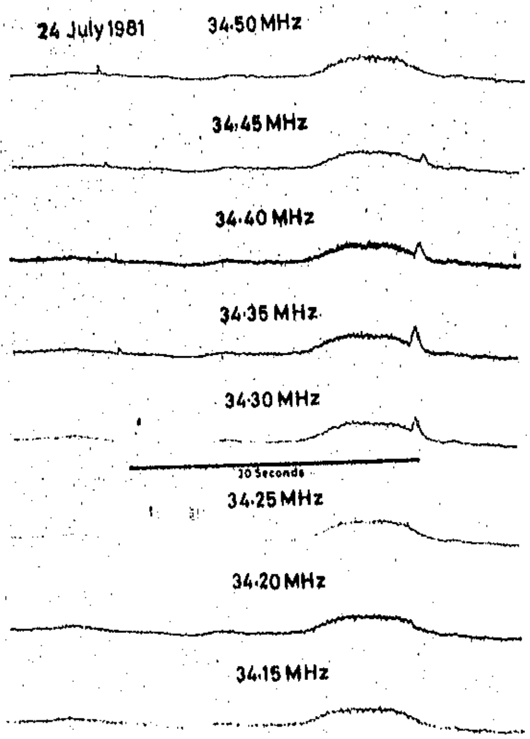

Fig. 3. Eight channel record obtained on July 24 1981. The ordinate is the intensity of radio emission.

(i) The frequency drift is very small which is ~250 KHZ S^{-1}.

(ii) The single frequency duration is ~300 ms.

(iii) The bandwidth is very narrow ~3%.

(iv) The single frequency duration increases with decreasing frequency. The total increase is ~100 ms.

(v) The bursts are superimposed over weak continuum.

The short duration narrow band bursts cannot be S-bursts (McConnel 1982) as the latter have very large drift rates. Though the drift rates are similar to type II bursts, one can rule out the possibility of type II because the type II's have a very large single frequency duration of several seconds. These bursts therefore have to be type I bursts. Since the occurence of closed magnetic fields in decametric region is relatively rare, the frequency of occurence of the type I bursts is also rare, which is consistent with the observations.

3.2. Interpretation

The bursts could not have been generated by electron cyclotron mechanism which is acceptable only when the plasma frequency is less than or close to the gyrofrequency of the electrons. The burst generation due to electron beam could also be ruled out because in this case the drift rates will be extremely large and contradict the observations. There is another possibility of getting the drift rate: a radio signal generated at a particular level is of finite extent in time. So, different Fourier components of the signal travel with different velocities because the refractive index is different for different frequencies. For such a process to be effective, a calculation of the dispersion measure shows that, the electron column density is extremely small and one may need six orders of magnitude more. Based on these facts one can clearly come to the conclusion that the bursts must be created by a weak shock wave moving out in the corona and can explain the observed slow drift.

Spicer et al. (1981) proposed the emerging flux theory to explain the type I bursts and the same thing is regarded as a working model (Wentzel 1982). The basic ingredients of the theory are two wave modes and a hot particle distribution. The high frequency wave mode is created by the hot particles. The low frequency mode produces the hot particle distribution by stochastic acceleration. The interaction between the two wave modes produces the radiation. The scenario is as follows. Newly emerging magnetic field pushes against the pre-existing coronal magnetic fields and produces shocks. In the shock front and its wake, a high level of lower hybrid (LH) waves are generated. Part of these LH waves stochastically accelerate electrons which are subsequently trapped in the closed magnetic arches and develop loss-cone anisotropy. The free energy in this electron distribution is fed into the upper hybrid waves (UH). A weak shock of slightly super Alfvénic velocity can generate the condition necessary for radio-emission and the drift rate of the bursts is the velocity of the shocks. The emerging flux theory can explain our observations. If the observed bursts are caused by a weak shock then the density jump across the shock should be directly related to the observed bandwidth. Therefore the observed bandwidth and the estimated shock velocity (from the drift rate) could be used in conjunction with the Rankine-Hugoniot relations to estimate the ambient magnetic field at decametric levels. The result is of the order of 1 G which is in very good agreement with other estimates such as frequency splitting and polarization measurements of type I bursts (ter Haar and Tsytovich 1980). This agreement is an indirect confirmation of the emerging flux theory in addition to some observational evidence provided by Karlicky and Jiricka (1982).

According to the emerging flux model, type I source is very tiny and the radiation is emitted instantaneously (Wentzel 1982).

The observed duration must be due to the finite extent of the generated radiation beam in which the rays making larger angle with the direction of the magnetic field lag behind those at smaller angles. This mechanism explains the short duration of the bursts. As the shock proceeds to lower frequencies, the extent of radiation beam may increase and also, there could be an increase in the range of angles in which the radiation is emitted. These two changes can cause increase in duration with decrease in frequency as observed. The weak continuum over which the bursts are superimposed must have been created by the interaction of UH waves with some unknown low frequency fluctuations.

In fact a weak shock can generate a variety of low and high frequency turbulences depending upon the strength of the shock and the coronal conditions which the shock faces as it propagates through the corona. The high frequency turbulence (Buneman Instability) is excited only at the initial portion of the shock front where the gradients are steep. Among low frequency waves, the LH waves are generated for isothermal conditions. The ion-sound waves are generated only when there is non-isothermality. Because of this the generation of ion-sound turbulence is always viewed with suspicion. But if there is an initial steep gradient, then the Buneman Instability generated can be quenched by essential heating of electrons and thereby causing non-isothermality (Tidman and Krall, 1971). In fact, the characteristic time scale for electron heating through Buneman instability is $\tau_B \simeq \sqrt{3}(m_e/m_i)^{1/3}\ \omega_{pe}^{-1} \sim 10^{-7}$s. This is very small compared to the shock transit time $(\omega_{pe} V_1/C)^{-1} \sim 5.8 \times 10^{-5}$s ($V_1$ - shock velocity). Hence the non-isothermality will be met within about 1/100th of the shock thickness. Under such a situation, therefore, ion-sound instability, could be excited. A detailed calculation of the ion-sound instability has been reported elsewhere (Gopalswamy et al. 1983b).

For the UH waves to provide the adequate brightness temperature, the low frequency waves should have an energy density (Melrose, 1980);

$$\frac{W^{\sigma}}{nT_e} \gtrsim \frac{6\sqrt{3}}{\pi} \quad \frac{V_e c}{\omega_{pe} L_n V_{ph}} ,$$

where

$\frac{W^{\sigma}}{nT_e}$ - energy density of low frequency mode σ interacting with the UH waves,

n - electron density of the corona

V_e - electron thermal velocity

V_{ph} - phase velocity of the low frequency waves

L_n - coronal density gradient scale length

c - velocity of light .

For $n = 10^8$ cm^{-3} and $T_e = 10^6$K, the above inequality becomes ;

$$\frac{W^{\sigma}}{nT_e} \gtrsim 2.4 \times 10^{-6} .$$

The energy density of LH waves is calculated by Spicer et al. (1981) as ;

$$\frac{W^{LH}}{nT_e} = \frac{\omega_{ce}^2}{\omega_{pe}^2} \quad \frac{V_A}{C_s} \quad \frac{\Delta B}{B} \quad \frac{M_A - 1}{M_A} \quad \left(\frac{m_e}{m_i}\right)^{1/2} ,$$

where V_A is Alfvén velocity, $\frac{\Delta B}{B}$ is the relative jump in magnetic field across the shock,

M_A is the Alfvénic Mach number, (m_e/m_i) is the ratio of electron to ion mass and C_s is the sound velocity. Following the similar procedure one can calculate the energy density of ion-sound waves by extending the one-dimensional calculation of Krall and Book (1969) to three dimensions (Gopalswamy et al. 1983b) as;

$$\frac{W^S}{nT_e} = \frac{C_s V_A}{V_e^2} \frac{\Delta B}{B} \frac{M_A^2 - 1}{M_A} \frac{2}{2-\beta} \left(\frac{m_i}{m_e}\right)^{1/2}$$

$$\times \left[1 + \ln \frac{\omega_{pe}^2}{\omega_{ce}^2}\right]^{-1} .$$

For identical conditions of the shock in the decametric corona,

$$\frac{W^{LH}}{nT_e} \simeq 7.7 \times 10^{-6} \quad \text{and} \quad \frac{W^S}{nT_e} \simeq 2.8 \times 10^{-4} ,$$

so that

$$\frac{W^{LH}}{W^S} \simeq 2.7 \times 10^{-2} .$$

This estimate shows that the LH waves only marginally satisfy the energy density requirement while the ion-sound wave density is much larger than the threshold value. Moreover, the ion-sound waves are generated over a wide range of wave numbers compared to that of LH waves, thereby satisfying the resonance condition more easily, i.e., the overlap between UH waves will be more in the case of ion-sound waves. Then, subject to the condition that the ion-sound waves are generated, they are better candidates compared to the LH waves.

Another important aspect of the emerging flux theory is the generation of UH waves. In the theory of Spicer et al. (1981), the LH waves stochastically accelerate the electrons parallel to the magnetic field. But UH waves are generated by a loss-cone distribution of electrons. Therefore, the accelerated electrons, travelling essentially parallel to the magnetic field should convert a major part of their parallel energy into perpendicular energy. Vlahos et al. (1982) have proposed anomalous Doppler resonance instability to generate a loss-cone distribution through pitch angle scattering. However, if the low frequency turbulence involved is due to ion-sound waves, there is another possibility of generating high frequency plasma turbulence. Since the ion-sound frequencies are of the same range as the whistlers, they can get non-linearly scattered into whistler waves in a time-scale of 0.01s (Kaplan & Tsytovich, 1973). The whistler polarization is such that the energy of the electrons is increased predominantly in the direction perpendicular to the magnetic field due to the whistler absorption. The time-scale over which the transverse energy of the electron increases is of the order of 0.5 s (Kaplan & Tsytovich, 1973). Since both these time scales are much less than the collisional damping time of the ion-sound waves, an anisotropic electron distribution could be produced, the free energy content of which could be fed into high frequency plasma oscillations through a mechanism similar to one discussed by Levin (1982).

In conclusion we would like to point out that while the emerging flux theory can adequately explain our observations as well as other type I phenomena, the low frequency models that provide the opacity could be different depending upon the exact conditions prevailing in the shocks and the corona.

4. Conclusions

We have presented some observations of the fine structures in the decametric solar radio emission. We have provided representative events which reflect the complex structure of the decametric corona. Our observations and their interpretations indicate the importance of this special region of the corona in understanding the radio physics of the Sun. As the decametric corona has not received much attention from theorists, a detailed investigation of the radio processes from this level will provide an opportunity for a better insight into outer corona as well as interplanetary phenomena.

References

Benz, A.O., and Kuijpers, J., 1976, Solar Phys. 46, 275.

Fokker, A.D., 1982, Solar Phys. 77, 255.

Galeev, A.A., 1976, in Physics of the Solar Planetary Environments, (ed. D.J.Williams) American Geophysical Union, 1, 464.

Gergely, T.E., and Kundu, M.R., 1975, Solar Phys. 41, 163.

Gopalswamy, N., Thejappa, G., and Sastry, Ch.V., 1983a, J. Astrophys. Astr. 4, 215.

Gopalswamy, N., Thejappa, G., Subramanian, K.R., and Sastry, Ch.V., 1983b, Presented at the IX A.S.I. meeting, Hyderabad.

Kaplan, S.A., and Tsytovich, V.N., 1973, Plasma Astrophysics: Pergamon, Oxford.

Karlicky, M. and Jiricka, K., 1982, Supplement to the Proceedings of 4th CESRA workshop on Solar Noise Storms (ed. A.O.Benz and P.Zlobec).

Krall, N.A., and Book, D.L., 1969, Phy. Fluids, 12, 347.

Kundu, M.R., 1982, Rep. Prog. Phys. 45, 1435.

Levin, B.N., 1982, Astron. Astrophys. 111, 71.

McConnel, D., 1982, Solar Phys. 78, 253.

Melrose, D.B., 1980, Solar Phys. 67, 357.

Sawant, H.S., 1982, in Solar Radio Storms, ed. A.O.Benz nd P.Zlobec, p.127.

Sastry, Ch.V., Subramanian, K.R., and Krishan, V., 1983, Astrophys. Lett. 23, 95.

Spicer, D.S., Benz, A.O., and Huba, H.D., 1981, Astron. Astrophys. 105, 221.

ter Haar, D., and Tsytovich, V.N., 1981, Phys. Rep. 73, 175.

Tidman, D.A., and Krall, N.A., 1971, Shock waves in collisionless plasmas, Interscience, New York.

Vlahos, L., Gergely, T.E., and Papadopoulos, K., 1982, Astrophys. J. 258, 812.

Wentzel, D.G., 1982, Proceedings of 4th CESRA Workshop on Solar Noise Storms (ed. A.O.Benz and P.Zlobech) Trieste, p.145.

DISCUSSION:

BHATTACHARYYA: In all the cases mentioned for absorption events did you find any suitable loop configuration from optical pictures?

GOPALSWAMY: Yes, that is what I was just discussing with Dr. R.N.Smartt. But, we have not specifically identified any event. He has promised to send some photographs in this regard. I am planning to search from our own optical records.

Kodaikanal Obs. Bull. (1984) 4, 55-56.

CONCLUDING DISCUSSION

R. Howard *
Mount Wilson and Las Campanas Observatories
Carnegie Institution of Washington
Pasadena, CA-91101, U.S.A.

The subject of this Colloquium is appropriate for the 75th anniversary of the discovery of the Evershed effect. It is also a timely and important subject. Today we have heard contributions on a variety of topics, and we have seen that there remain a number of important unsolved questions. We have learnt a great deal about the interaction of plasma and magnetic fields in recent decades, but the phenomena of the solar atmosphere continue to defy physical explanation and their field remain as challenging as the day 75 years ago when Evershed discovered motions in sunspots.

Mathematical modelling of the small scale magnetic structures of the solar atmosphere is leading to more accurate physical descriptions of such features, but at the same time the refinements in such analyses, as we have seen here today, bring with them the necessity for more detailed, high resolution observations of the solar surface. The promise of a quantum jump in spatial resolution from space observations lies still in the distant future, so far now the best efforts of ground-based observers will be needed to aid the theoreticians. Today we have heard from both theoreticians and observers, and we see that progress is reported from both groups. Meeting such as this which bring together these researchers are valuable means of advancing the field.

The nature of the solar activity cycle remains one of the most puzzling questions in solar physics. Today, we have heard a fine review of this field and an interesting new model has been proposed. Few areas of astronomy have seen such a long and heated debate as that of the solar dynamo. In recent years the stellar astronomers have joined the fray with observations of stellar cycles. This has added a valuable new dimension to the subject. Today we saw observations relating to the cycle and one is tempted to suggest that although new observations are always desirable, in this field we may have too many observations. That is, the interaction has the difficult job of relating those large scale, long term phenomena that are truly relevant to the fundamental cycle mechanism and discarding those that are only incidental to the important physics of the process. It may be that we have already in hand the key to the solution of the cycle, if we only knew what it was and don't mean to suggest that we should stop observing large scale phenomena. Clearly the search must continue until we can make further progress. Currently the kinematic dynamo models are favoured

---

* Presently at National Solar Observatory, Tucson, Arizona, U.S.A. Operated by the Association of Universities for Research in Astronomy, Inc. under contract with the National Science Foundation.

by many who have worked on them. But, as we have seen today, they have their weaknesses and many people feel that we must look elsewhere for a cycle mechanism. The search continues.

It is appropriate that at this meeting we have heard a good review about the Evershed effect. We seem to have made little progress in understanding this phenomena in 75 years, and after all this time we are still faced with observations that seem contradictory. Of course perhaps not all sunspots show the same dynamical properties, but if this is the case, then we can add a further puzzling dimension to the Evershed effect. The very highest possible spatial resolution is required to study the motions in sunspots. This is another field where a breakthrough may be anticipated when sub arc-second observations from space become available. In this case, as in others, we need high resolution velocity, magnetic field, and brightness information with extended coverage in time (at least some hours). Until such space observations become possible, and in fact, in preparation for them, we should use modern ground-based techniques to define better the dynamical properties of sunspots. In particular, it seems to me, differences in the amplitude or form of the Evershed effect should be investigated. Are such irregularities related to the size, shape or age of the spots? What form does the Evershed effect take for irregularly shaped penumbrae? The answers to questions such as these can be obtained from the ground and should precede space observations.

We work in an exciting field that does not lack for important unsolved questions. Among these are the nature of small scale motions in sunspots and elsewhere on the solar surface and the fundamental mechanism of the solar cycle. An important start in the study of these processes was made 75 years ago here by Evershed, and the opportunities for significant advances in our knowledge of these topics is even greater today than it was then.